Planktonic Larval Fin & Shellfish Ingress
&
Vertical Distribution in the Aransas Pass Inlet System

Publication CBBEP – 167
Project Number – 2125
August 2023

Prepared by

David Portnoy
Olivia Robson, BS

Edited by
Simon Geist

Texas A&M University – Corpus Christi
6300 Ocean Drive, Unit 5800
Corpus Christi, Texas 78412

Submitted to:
Coastal Bend Bays & Estuaries Program
1305 N Shoreline Blvd, Suite 205
Corpus Christi, TX 78401

Planktonic Larval Fin & Shellfish Ingress
&
Vertical Distribution in the Aransas Pass Inlet System

Contract Number 2125

PROJECT COORDINATOR
Cherie McCollough, Ph. D
Texas A&M University-Corpus Christi Tidal Hall 309F
6300 Ocean Drive, Unit 5800 Corpus Christi, Texas 78412-5800
Phone: 361-825-3166
E-mail:

CBBEP Project Manager
Rosario Martinez

Final Report
August 10, 2023

Submitted to:
Coastal Bend & Estuaries Program
1305 N. Shoreline Blvd., Suite 205
Corpus Christi, TX 78401

Prepared by
David Portnoy
Olivia Robson, BS
Edited by:
S. Geist

Executive Summary

Estuaries, such as coastal bays and lagoons, provide important nursery ground for juvenile fishes and shellfish and many are connected to the ocean via inlets. Larval stages of fish (Ichthyoplankton) and shellfish species must pass though these inlets that act as a bottleneck for the transport of larvae from their oceanic spawning grounds to estuarine nursery habitats. Larval fish (Ichthyoplankton) have limited horizontal swimming capabilities against strong currents, which often occur in coastal inlets, and thus rely heavily on water currents for transport which they can detect using environmental cues and reach by vertically positioning themselves in the water column. In recent years, desalination plants have become a sought-after source of drinking water in the United States. While increasing access to a much-needed resource, desalination plants can have harmful effects on the coastal marine environment. Desalination plant intakes kill larvae by impingement and entrainment, and discharge of salt brine alters the salt content in the vicinity of the outflow, together with elevated water temperature and elevated concentrations of heavy metals and other toxic elements. In the spatially confined setting of a coastal inlet with limited space to avoid the impacted zones, the risk that larval fish are negatively affected by these multiple, parallel stressors associated with desalination plant may be high. This study investigated ichthyoplankton abundance in the Aransas Pass Inlet system by sampling the Inlet and the three different channels that make up the System (Corpus Christi Ship Channel, Aransas Pass Channel, Lydia Ann Channel) in different water depths to improve our understanding how larvae use the inlet waters as they pass from the Gulf of Mexico to their nursery habitats in the Aransas-Corpus Christi Bay System. A total of 17,645 fish were identified to one of 22 families and an additional 400 individuals could not be identified to family but were identified as the

ordinal level across six months, solidifying the fact that the Port Aransas Inlet is an important area for larval ingress with a large diversity of fishes. Larval density was found to statistically increase or decrease with some the factors tested, most notable being photoperiod and month. Furthermore, family level analysis showed differing correlation between family density and the factors tested. Sciaenid (drums) density was highest during the months of October and November, while increased sparid (porgies) densities occurred in February. The analysis of environmental drivers of ichthyoplankton density provide information for planning purpose that will allow better mitigation and reduction of the effects of anthropogenic activities, specifically in this case the implementation and construction of a desalination plant located on Harbor Island. Through restricting timing and location of discharge and intake flows of the desalination plant the negative impacts on the susceptible ichthyoplankton can be reduced.

Table of Contents

Introduction

Estuaries, such as coastal bays and lagoons, provide important nursery ground for juvenile fishes and shellfish. This essential habitat is structurally complex and provides protection for juvenile fish from predators and provide foraging opportunities increasing the chance of survivorship (Minello 1999). Inlets are a prominent feature of many coastal waterways that connect the ocean to estuaries and are dynamic environments with distinct seasonal changes in environmental parameters, such as water temperature, salinity and dissolved oxygen concentration. Larval stages of many fish and shellfish species must pass though inlets, which act as a bottleneck for the transport of larvae from their oceanic spawning grounds to nursery habitat (Boehlert & Mundy 1988, Schieler et al. 2014). Anthropogenic factors such as increased turbidity from boating activity and artificial light can disorient larvae and reduce the rate of successful ingress into estuaries (Collin & Hart 2015). To better understand spatiotemporal patterns of ichthyoplankton ingress it is crucial to understand 1) the composition of ichthyoplankton, 2) their spatial distribution in the water column, 3) shifts in composition and distribution over time, and 4) what environmental factors correspond with shifts in composition. All four components help us to understand patterns of larval ingress and thus allowing us to engage in planning to mitigate the human impacts.

In Texas coastal recreational sportfishing accounts for $1.79 billion each year, with most funds being attributed to red drum fishing (Southwick 2006). While some species spend their entire life history in estuaries, like many species of gobiids, this research will put special focus on estuarine-dependent, marine species that use estuaries as nursery grounds during their early life stages. These obligate estuarine-dependent marine fishes are species that require an estuary for part of their life cycle and can either spawn in the estuary and move offshore as they age or

spawn offshore and move into the estuary for their larval stage (Able 2005). Because this research focusses on movement of larvae through inlets, the fish species which spawn offshore in the Gulf of Mexico (GOM) and move into estuaries for nursery habitat will be the primary focus. Since ichthyoplankton have limited horizontal swimming capabilities against strong currents, which often occur in coastal inlets, they are thought to rely heavily on environmental cues and position in the water column for transport in and out of the protected waters. Major cues that can affect ingress include seasonal temperature change, tidal variation, and daylight duration (Wiseman Jr. & Dinnel 1988). There are two primary mechanisms of larval transport through inlets: one being passive and the other being active transport.

Passive transport models view planktonic larvae as passive particles which are solely moved by physical forces. Some studies use 2 or 3-dimension models in which the larval planktonic organisms do not respond to any environmental cues and are akin to passive particles like grains of sand or pieces of plastic (Pietrafesa et al. 1988, Seabergh 1988, and Wang 1988). These models are heavily driven by three components: wind, tidal fluxes, and physical geography of the estuary. Additionally, inlet and current velocity and overall water flow are the main elements being modeled. Tidal flow creates a plume of estuarine water in the marine environment during the ebb tide and a plume of ocean water in the estuary during the flood tide. Passive transport studies characterize tidal plumes as the major transport mechanism into and out of an estuary (Pietrafesa et al. 1988, Seabergh 1988, and Wang 1988). The tidal changes and transport currents can also be affected by wind velocity, which is often a key factor in estuaries in the eastern GOM (Brown et al. 2005). While modeling larvae as passive particles provides a good basis for understanding complex physical transport through costal inlets, it is seen as an incomplete representation by many in the scientific community today (Whitefield et al. 2023).

Active transport models view planktonic larvae not as passive particles but as active individuals responding to cues in the environment. More recent studies, such as Faillettaz et al (2018), have found that including simple swimming behavior in dispersion models increases accuracy as compared to passive larval models. Many studies have shown evidence of behavioral responses to the environmental cues involved in current fluctuations (Boehlert & Mundy 1988, Baptista et al. 2020). Vertical migration is known to occur in planktonic species; with plankton moving up in the water column at night and down during the day to avoid predators and/or harsh UV rays, or to seek food items. There is some evidence that ichthyoplankton use vertical movement as a way of transport through inlets (Schieler et al. 2014, Whitfield et al. 2023, Wenner et al. 2005). In their review, Boehlert & Mundy (1988) found that the use of vertical movements to facilitate transport through inlets was highly variable among species (Figure 1). *Paralichthys* spp. in North Carolina were found in higher concentration on flood tides during the night as compared to ebb tide during the day, leading Weinstein et al. (1980) to speculate that post larval flounder shifted to the bottom during ebb tides (Figure 1.) By comparison, Weinstein et al. (1980) found that Atlantic croaker, (*Micropogonias undulatus*), remained deeper in the water column both day and night (Figure 1). Boehlert & Mundy (1980) assert clear evidence for behavioral responses to tidal forces but what cues these responses is less clear. There is evidence for light level affecting water column position of plankton, but there are also other cues such as salinity. In their study, Téodosio et al. (2016) present the Sense Acuity and Behavioral (SAAB) hypothesis which states that ichthyoplankton use a hierarchy of cues including odor, sound, visual, and geomagnetic. The SAAB hypothesis has two components, offshore and nearshore components, and is based on studies of post-flexion larvae across multiple temperate species. When larvae are offshore, the SAAB hypothesis maintains that they use cues from sensory organs that detect the sun's intensity

and position and earth's geomagnetic field. Nearshore the larvae will exhibit behaviors in response to estuarian cues such as odor, sound, and visual cues. Baptista et al. (2020), found that both post and pre-flexion white seabream *(Diplodus sargus*) larvae can swim at speeds greater than most ocean currents, showing that these larvae are not restricted to passive dispersal. Salinity cues have been most apparent in shrimp and crab species (Boehlert and Mundy 1980), which have been shown to be recruit, transition into juveniles, more successfully in years with high rainfall (Boehlert and Mundy 1980). Salinity cues are particularly important for this research because as human water usage increases while freshwater stores decrease, desalination plants and their effluents will apply more pressure to coastal ecosystems. The salinity will increase wherever the briny discharge of a desalination plant is located in the estuary and can be further exasperated by slow flushing times and bottom topography. The high levels of salinity would not only cause osmotic stress on the organisms but may interfere with inlet transport cues.

The Aransas Pass Inlet system connects the GOM waters with several bays: Aransas Bay, Corpus Christi Bay, Nueces Bay, Redfish Bay, Copano Bay, and St Charles Bay. The nearest natural inlets are 35 km north and 125 km south (Pass Cavallo and Mansfield Pass respectively) and a much smaller artificial inlet is 29 km south (Packery Channel) of the Aransas Pass Inlet, making the Aransas Pass Inlet an important, major point of ingress (and bottle neck) for larval fish and shellfish to reach nursery habitat. Even though larval stages are crucial in the life history of many marine species, only a few studies have been conducted in the geographic area, with knowledge of the vertical distribution of larvae in the water column being scarce. In shallow coastal estuaries such as Aransas Bay and Corpus Christi Bay, wind and tidal forcing are the two key physical components (Brown et al. 2005). Brown et al.'s (2005) 2-dimensional model showed high accuracy for predicting pulses of larval recruitment, with solely physical passive

transport data. When models with and without wind forcing were compared, wind forcing could at least partially account for increases in particles into Aransas Bay (Brown et al. 2005). However, that study simplified the Bay system and lacked the complex bathymetry required. In another study, Holt & Holt (2000) found that during the day the concentration of larvae was higher in bottom tows, while at night the number of larvae was consistent throughout the water column, indicating a relationship between photoperiod and depth. The differing densities of ichthyoplankton at varying depths supports the SAAB hypothesis. The conclusion of these studies is somewhat limited, however, because they focused on only two species, red drum (*Sciaenops ocellatus*) and spotted seatrout (*Cynoscion nebulosus*) and were limited to Lydia Ann Channel and a period of six weeks of sampling in late summer/early fall (Holt & Holt 2000). A more recent and comprehensive study of blue crab larvae (megalops) found the highest amount of blue crab megalops in their GOM and Aransas Pass Inlet sampling sites during the months of October and February (Weatherall et al. 2018). However, this study was focused on only settlement stage larvae gathered with an artificial substrate collector, which only gives insight into a small proportion of the population. Information on planktonic larvae of other commercially important species in the Aransas Bay area is lacking. However, the importance of adjacent bay systems as nursery areas is well known and documented by regular bag seine monitoring of fingerling-sized juveniles by the Texas Parks and Wildlife Department Coastal Fisheries and a parallel study on newly settled juvenile fish stages sampled with an epibenthic sled that documented 30 fish and nine crustacean taxa in the inlet area (Stunz et al. 2022).

In recent years desalination plants have become a sought-after source of freshwater in coastal regions of the United States (Rao et al. 2018). While increasing access to a much-needed resource, desalination plants can have harmful effects on the coastal marine environment.

Desalination plants intake seawater, through various methods, remove the salt, and discharge a briny solution back into the coastal environment. Both the intake and discharge of seawater by desalinations plants can be detrimental to marine fauna (Missimer & Maliva 2018, Miri & Chouikhi 2005, Petersen et al 2018). Intake systems can cause impingement, entrapment, and entrainment of smaller marine organisms, particularly larvae and eggs, and as result kill them. The mitigation of velocity and implementation of protective mesh screen coverings for intake heads has been shown to reduce the effects of entrapment (Missimer & Maliva 2018, Petersen et al. 2018). The discharge of brine effluent is perhaps more harmful, as brine not only increases the surrounding salinity, but it can change temperature, elevate heavy metal concentrations, and discharge harmful antifouling chemicals (Miri & Chouikhi 2005).A diffuser can be used to dilute the brine effluents and prevent accumulation on the seafloor (Missimer et al. 2018), but at the same time it creates a larger plume and increases the volume of affected water. Depending on the spatial settings and especially in a confined inlet channel, this may lead to a situation where most larvae cannot avoid getting in contact with this plume water during their passage. An increase in temperature and salinity is associated with lower oxygen solubility in water, increased physiological stress on fishes, and increased turbidity of seawater (Miri & Chouikhi 2005). Abrupt changes in salinity have been known to affect species growth differently, with an increase in salinity slowing growth rate in *Micropogonias undulatus* (Peterson et al. 1999) and increasing growth rate in *Paralichthys lethostigma* (Moustakas et al. 2004). Although, a study by Specker et al. (1999), also tested *P. lethostigma* growth and survivorship at different salinities and found that at 38 ppt *P. lethostigma* may result in slowed growth rates while lower salinities (8 ppt and 14 ppt) showed no adverse effects. Turbidity can perhaps create both positive and negative conditions for ichthyoplankton; increasing the ability to hide from predation (Fisken et

al. 2002, Carreon-Martinez et al., 2014) but decreasing their ability to detect prey (Salonen et al., 2009). Anti-fouling chemicals increase toxicity and are known to impact fish embryo development (Petersen et al. 2018) and cause increased physiological stress. These factors can not only harm the individual larva, but they can also be detrimental to their food sources, reducing the number of zooplankton and thus reducing their chances of feeding success. The growth-survival paradigm, first introduced by Anderson (1988), suggests that slower growing individuals have a reduced chance of survival as they remain in the larval stage longer and are thus more susceptible to starvation and predation (Pepin et al. 2014).

There are several proposed desalination plants in the coastal Texas area, including a proposed desalination plant on Harbor Island, Port Aransas TX with both an inflow and an outflow diffuser located in the coastal inlet channel near the geographic focus of this study. (Figure 2). Unfortunately, few published studies have assessed the potential impacts of these plants on subtropical waters as seen in coastal Texas, not to mention with in- and outflow located in a coastal inlet or an estuarine bay.

Therefore, the main objective of this study was to identify patterns of larval transport through the Port Aransas Inlet System to better estimate the risk for encountering impacts of the proposed desalination plant and other future development projects. As the reproductive seasons differ among species, different fish families and species were sampled in the Port Aransas Inlet system during the months of June 2021, July 2021, September 2021, October 2021, November 2021, and February 2022, and including their vertical position in the water column using a depth stratified sampling design. In addition, we sought to investigate factors influencing larval transport in the Port Aransas Channel system, as example for an inlet into mixed estuaries, including tide, time of day, and time of year. Taken together, this study will provide critical data

for risk management assessment as it pertains to the effects of the proposed Harbor Island desalination plant on the ichthyofauna of the Aransas-Corpus Christi Bay System.

Methods

Field Sampling

Three channels comprise the Aransas Pass Inlet System: Lydia Ann Channel, Aransas Pass Channel, and Corpus Christi Shipping Channel. The largest, Corpus Christi Ship Channel, is approximately 13.7 meters deep by 121.9 meters wide and acts as the main pathway for large cargo and tanker vessels traveling to the Port of Corpus Christi. There are ongoing plans to increase Corpus Christi Ship Channel to 16.5 meters deep and 161.5 meters wide (Torres 2020). The Aransas Pass Channel is approximately 14.3 meters deep and 40 meters wide, with proposals for dredging and extending the channel into the Gulf of Mexico (Brown et al. 2005). Lydia Ann Channel is approximately 7.6 meters deep and 250 meters wide at the entrance narrowing to 4 meters deep and 40 meters wide near the exit to Aransas Bay (Brown et al. 2005). The Corpus Christi Ship Channel, accounts for 60% of the water flow from the Gulf of Mexico (Brown et al. 2005) into the Aransas Bay System. The tides in the area are diurnal to mixed diurnal-semidiurnal (Brown et al 2005) and are highly wind driven. The bottom of all three channels mainly consists of sand and silt, with seagrass beds compromising 11% of the bottom of the surrounding bays and the majority of seagrass occurring in Redfish Bay (Brown et al. 2005).

To assess ichthyoplanktonic composition/density a sampling site was located in each channel (Aransas Pass Inlet, AP1; Corpus Christi Ship Channel, CC1; and Lydia Ann Channel, LA1 on Figure 2) with a fourth being located in between the jetties of the Inlet itself (Port Aransas Channel; PA1 located on Figure 2). Sampling occurred over the course of several months

starting in June of 2021 and ending in February of 2022 to account for seasonal differences in spawning activity among fishes.

Both ingoing and outgoing tides were sampled for a comparative analysis of passive and active transport of the plankton. Samples were also collected during daylight and nighttime hours, as previous studies have shown the importance of diurnal vertical movement (Holt & Holt 2000). Lastly, 2-3 discrete depths were sampled (depending on the average depth of the channel; 3 depths for CC1 & PA1 and 2 depths for AP1 & LA1) as ichthyoplankton are known to move horizontally in the water column depending on photoperiod and tide. The Pythagorean theorem was used to calculate the amount of tow line needed for the desired depth of sampling as described in the NOAA SEAMAP Operations Manual (2001). An ideal angle of 45 degrees was used in the equation along with total depth and desired depth. The tow line was marked in one- and five-meter increments and quickly lowered to desired depth using a winch system. The line angle was continually measured during the tow to ensure stability around 45 degrees. A total of 13 sampling days were completed with every combination of site, photoperiod, tidal phase, and depth strata occurring, with exceptions due to poor weather conditions or high levels of marine traffic.

Each sample was collected using a ring net (75 cm diameter, 500 μm mesh width, 5:1 diameter length ratio) equipped with a mechanical flow meter (General Oceanics). The initial tow occurred just below the surface, the second mid water column, and the final tow just above the seafloor (all depending on total depth of the station). The net was towed for 3-10 minutes, depending on time of day (photoperiod), at 1-2 knots for a goal of 100 m^3 of water volume sampled per net tow. All samples were initially preserved in a 50% ethanol solution, then filtered and stored in 100% ethanol within 24 hours of collection. For processing in the lab, plankton

samples were split if necessary (total of two subsamples) and subsamples were used to quantify larvae. All ichthyoplankton were identified to the family level, with most sciaenids being identified to genus and species when possible. *Menticirrhus* sp. were combined into one group due to the difficulty of accurately differentiating among M*enticirrhus americanus* (southern kingfish), *M. littoralis* (Gulf kingfish), and *M. saxaltilis* (northern kingfish). For larvae where it was hard to identify species and of particular importance, DNA Barcoding was used to verify identification. Paralichthyids were identified to genus and species level using DNA barcoding as they cannot be reliably identified solely on morphological characteristics. The following species were identified in the barcoding of paralichthyids: *Paralichthys lethostigma* (southern flounder), *Paralichthys albigutta* (Gulf flounder), and *Citharichthys spilopterus* (bay whiff). All individuals classified as unknown were considered in too poor condition to be accurately identified by morphological characteristics. Larval density was calculated using the following equation for the water volume:

$$Filtered\ water\ volume = \pi \times r^2 \times \frac{(Flowmeter\ final - flowmeter\ initial) \times 26873}{999{,}999}$$

with r = the radius of the net opening and 26873 = rotor constant for the flowmeter (General Oceanics Inc, 2018).

Environmental variables

During each sampling day and at every station, temperature, salinity, pH, and O_2 concentration profiles were taken using a multiparameter sonde (YSI exo1 or YSI V2). These measurements were collected once per photoperiod and tidal change, by slowly lowering the device through the water column. A sampling event consisting of samples taken for ingoing and outgoing tide once

during night hours and once during day light hours. NOAA buoy water quality measurements were taken for the sampling done in September due to equipment difficulties.

Ichthyoplankton Community Analysis

Total larval density of each sample was calculated with the following equation:

$$Total\ larval\ density\ (fish\ per\ 100m^3) = \frac{fish\ count}{filtered\ water\ volume} \times 100$$

All analysis was completed in R and R Studio using the *gls* (generalized least squares) function in the package *nlme* (V4.1.1; Hankin 2006, Pinheiro et al. 2021, R Core Team 2021, RStudio Team 2020). A full model with 2-way interactions included was used to compare total larval density for each sample with time of day, tide, net depth, and month. The factor, season, was removed as it repeated the factor of month, and 3-way interactions were not included as they are extremely complex and would result in little interpretable results. The sampling completed in June and July was removed from this analysis as outgoing tide was not sampled during those dates. An analysis of the distribution of larval density across all samples showed that the residuals were non-normally distributed with a biological wall at 0 fish/100m^3 and a long upper tail, to account for this total larval density was then log transformed. GLS analysis was chosen as it is best suited for a continuous variable and can be used to compare the interactions between factors.

Family-level Analyses

Family level diversity analysis was completed with the same methods as the analysis for the total larval density. The families Sciaenidae and Paralichthyidae were chosen based on their economic importance and their spawning migratory behavior. Only Fall, the peak spawning season, was

analyzed for the Sciaenidae to reduce the amount of zero values (ties) and to focus on spawning time. The residuals of the larval density data for Sciaenidae family were not normal even after log transforming the data, so the ANOVA results were verified using a Wilcoxon rank sum exact test.

A Principal component analysis (PCA) was conducted to explore the correlation between the ichthyoplankton community (family level) and the environmental variables, tide, depth, photoperiod, and month. Analysis was performed in R and R Studio using the *prcomp* function. Scree plot was created using *factoextra* package (V1.0.7 Kassambara & Mundt 2020). The first, second, third, and fourth principal component axes were used to assess community as they accounted for a sum of 99.6% of the variation (Figure 12). Four families (Sciaenidae, Gobiidae, Clupeidae, and Sparidae) which accounted for the highest correlation to each principal component were the focus of the analysis (Figure 13, Figure 14, Figure 15, Figure 16).

Over 93% of the sciaenid individuals collected were identified as *Micropogonias undulatus*, which left little data for complete analysis of each sciaenid species. Thus, sciaenid species density was not individually analyzed and *Sciaenidae* family analysis was understood to be driven by *M. undulatus.*

As the majority of paralichthyids identified in the samples are *Citharichthys spilopterus* (bay whiff), which spend their life cycle in bays and estuaries, the paralichthyids were not analyzed on a family level. This study's aim was to explore the differences in larval densities of species whose adults migrate offshore to spawn and whose larvae are transported into the bays and estuaries for nursery habitat. Furthermore, barcoding resulted in a high level of inaccuracy when identifying to species, so the authors did not feel comfortable with further analysis until barcoding could be completed for all individuals.

Results

Environmental variables

Across all samples, pH levels were consistent ranging from 7.5 to 8.4 and remained mixed within a sample. Both the highest and lowest pH levels were found at station LA1 June had the highest salinities measured and the warmest temperatures measured (Figure 3). The coolest temperatures were measured in February and the lowest salinities were recorded in October (Figure 3).

During summer, water quality data was collected in June only, not July, as the sampling for June and July was considered one sampling session. The average temperature in June ranged from 25 to 30 °C. Stations AP1NI and CC1NI both showed stratification between warmer surface waters and cooler waters as depth increased. Salinity ranged from 28 to 38 and was the highest salinity measured for all months. Similarly, to the temperature measurements, stations AP1NI and CC1NI showed stratification with lower salinity measurements at the surface and increasing salinity with depth. Dissolved oxygen (DO) concentrations were consistent throughout the water column for stations PA1DI and PA1NI, approximately 5.5 mg/L and 4 mg/L respectively. Stations AP1NI and CC1NI showed stratification with higher DO concentrations at the surface, 5-6 mg/L, and decreasing concentration with an increase in depth (Figure 4).

In October, the average temperature ranged from 25 to 28 °C varying by station, with complete mixing of the water column an example can be seen in Figure 3 C. Figure 3 D, display the average salinity for the month of October, but there are a few exceptions in which the surface waters display a slight stratification from the rest of the water column. The stations with semi stratified salinities have a surface layer of water with lower salinities, of on average 22, and an increasing salinity measurement with depth. The stations with semi stratified waters include PA1DO, LA1NO, LA1NI, LA1DO, CC1NI, CC1DO, CCDI, and AP1NI (Figures 3 D).

Dissolved oxygen concentrations for the month of October ranged from 6 to 8 mg/L throughout the water columns for all stations (Figure 4).

November water temperatures ranged from 22 to 24 °C (Figure 3 E) and showed consistent mixing across all stations. Most stations in November showed consistent salinities as well with an approximate salinity 34, (Figure 3 F). Salinity was stratified in only one station, LA1, for three of the samples, LA1DI (slack), LA1DO, and LA1NI, this month seen in Figure 3 F. Dissolved oxygen concentrations ranged from 6.5 to 7.7 mg/L for all stations and remained mixed within stations (Figure 4).

During February water temperatures ranged from 11 to 13 °C with complete vertical mixing for all stations (Figure 3 G). Salinity for most stations was vertically mixed ranging from 31 to 32 (Figure 3 H). Salinity was semi stratified for stations LA1DI, AP1DI, PADI, and PA1NI, seen in Figure 3 H. Dissolved oxygen concentrations for February ranged from 9 to 10 mg/L for all stations and were mixed within stations (Figure 4).

For September water quality data was collected from a NOAA buoy station due to an error in data collection. Corpus Christi Channel at the approximate location of CC1 water temperature ranged 30 to 31 °C at the surface waters, Figure 5. This buoy is located on the southern edge of the channel unlike CC1 which was center of the channel and only has data from the surface waters, not a complete profile. Salinity, pH, and oxygen concentration data for this month were unavailable.

Ichthyoplankton Community Analysis

A total of 150 net tows were completed over the course of 11 days and across six months: June, July, September, October, November, and February in 2021/2022. 18,076 ichthyoplankton were collected, and total larval densities ranged from 0 to 1141.76 Ind./100m^3 in individual net hauls.

A total of 17,645 fish were identified to one of 22 families and an additional 400 individuals could not be identified to family but were identified as the ordinal level (Tables 1-4). Thirty-one individual larvae were not identified due to poor condition. Numerically dominant families for every sampling month included the Sciaenidae, Clupeidae, and Gobiidae. The most abundant families differed based on factors, month, time of day, tidal cycle, and net depth. In the month of September, engraulids (5.91 fish/100m^2) were abundant and had similar concentrations as clupeids (6.74 fish/100m^2) (Table 1). Sciaenids were most abundant in October and November, with concentrations up to five times greater than the concentrations of other families (Table 1). February saw a decrease in the concentration of sciaenids with the sparids and clupeids being the most abundant (Table 1). During the day sparids and clupeids were the most abundant families, while during the night sciaenids and gobiids were the most abundant (Table 2). Sciaenids, gobiids, and clupeids were consistently abundant across both tidal cycles, while sparids were noticeably more abundant during the outgoing tide (Table 3). Sparids were also more abundant at non-surface depths than surface depths (Table 4).

The majority of sciaenids were identified to species level with seven species total identified: *Cynoscion arenarius* (sand seatrout), *Cynoscion nebulosus* (spotted seatrout), *Cynoscion nothus* (silver seatrout), *Larimus fasciatus* (banded drum), *Menticirrhus americanus* (southern kingfish), *Micropogonias undulatus* (Atlantic croaker), *Sciaenops ocellatus* (red drum) (Table 5-8). For the months of October and November *M. undulatus* had the largest larval densities (Table 5). The densities for *M. undulatus* were approximately ten times greater than the densities for the

next most abundant species, *S. ocellatus* in October and over two hundred times larger than *Menticirrhus spp.* in November (Table 5). *M. undulatus* had higher densities during night, non-surface depth, and ingoing tides (Tables 6-8). Although they did not display a large difference in density based on net depth, *S. ocellatus* had larger densities during night hours and outgoing tides (Tables 6-8).

Out of 19 individuals barcoded, 12 were correctly identified to species, seen below in Table 9. As only 63% were correctly speciated using morphological characteristics further analysis was not completed. Although future barcoding may be completed on all individuals identified as *Paralichthys* for a later analysis.

The initial model compared total larval density against the four factors tidal cycle, time of day, depth, and month; and resulted in time of day having the highest *f*-value (35.2) indicating the largest group separation. (Table 10). The model was then split into day only and night only to better understand fine scale patterns within each group. The distribution of the total larval density for each month sampled is significantly larger at night than during the day (Figure 6). The variation between day night is most apparent in fall months and less apparent in February (Figure 6).

The day-only model resulted in a significant interaction between month and tide thus the day model was split into a one-way model of tide by month (Table 11). Only the months of September ($p < 0.01$) and February ($p < 0.05$) had significant differences between tides (Table 12). In September ingoing tide had significantly higher densities than outgoing tide, while in February outgoing tide had significantly higher densities (Figure 7).

The night-only model resulted in a significant interaction between month and depth stratum, thus the day model was split into a one-way model of depth stratum by month (Table 13). Tide was not included in the night model because of non-significance, which may be due to insufficient sample size. During the months of September, October, and November the non-surface samples had significantly higher densities than the surface samples while in February the surface samples had significantly higher densities (Figure 9). Month and depth stratum had a significant interaction ($p < 0.005$; Table 14; Figure 8).

Family-level Analyses

The sciaenid model showed a significance relationship in larval density with factors time of day and the interaction between time of day and depth (Table 15). The Sciaenidae model was then broken down into a day-time model and night-time model as that factor had the largest *f*-value (75.772) and thus indicating the most group separation. There was a significant difference ($p< 0.05$) in larval density due to the interaction between time of day and depth. As seen in Tables 5 – 8, the majority of identified sciaenids were *M. undulatus* (Atlantic croaker) indicating that the results of the sciaenid analysis are driven by *M. undulatus*, with higher larval densities occurring at night and non-surface depths (Figure 9).

The day model showed a significant difference in larval density based on depth, with higher larval densities occurring at non-surface depths (mid and bottom tows) (Table 16). This difference was consistent across both ingoing and outgoing tides but is more apparent during the outgoing tide (Figure 10). There was no significant interaction between tide and depth.

The night-only Sciaenidae model shows a significant difference ($\alpha < 0.05$, Table 17) in larval density based on the interaction between tide and depth, with higher densities occurring at non-surface depths for both tidal cycles but only significantly higher densities occurring during outgoing tide for non-surface depths (Figure 11).

An increase in sciaenid density is positively correlated with the months October and November, while an increase in clupeid density is positively correlated with the month October and an increase in sparid density with February (Figure 17, Figure 18). Gobiid density has a possible positive correlation with September, but the correlation is not as apparent as with the other families (Figure 17, Figure 18). There is little correlation between tidal cycle and family densities, although there is an increase in sparid density associated with outgoing tide (Figure 19, Figure 20). All four families (Sciaenidae, Clupeidae, Gobiidae, and Sparidae) have a positive correlation between family density and night (Figure 21, Figure 22). Sciaenid, Clupeid, and Gobiid densities are positively correlated with non-surface depths, while Sparid density is positively correlated with surface depths (Figure 23, Figure 24).

Discussion

Ichthyoplankton Transportation

This study focused on transportation of larvae which spawn offshore and migrate inshore for nursery habitat, primarily sciaenids and paralichthyids (southern flounder). While several individuals were identified as *P. lethostigma*, unfortunately the number was not large enough to do a robust statistical analysis (ANOVA) as was the case with the sciaenids. Targeting the spawning timeframe of *P. lethostigma* would make a more ideal data set for analysis. With these factors in mind, the interpretation of the results will focus primarily on the months (October and

November) and during night hours, in which sciaenids were found to be the most abundant family. Analysis of total larval density indicated higher densities at night and during the months of October and November. During the day density varied based on the interaction of month and tide, while during the night density varied based on the interaction between month and depth. The total larval density during the months of October and November was driven by the sciaenids with significantly higher densities of sciaenids occurring at night and lower in the water column (non-surface depths).

Significantly lower larval fish densities during daylight hours were also found in a prior at Packery Channel, Corpus Christi (Bromschwig, 2019) and may indicate a predator avoidance strategy and/or avoidance of damaging UV rays. Both theories are commonly referred to when discussing diel vertical migration (DVM; Lampert 1989, Hays 2003). Although, this study found significantly higher total larval densities at night occurred in non-surface waters (September, October, and November) and no significant differences in total larval density through depth during the day, which does not align with DVM. However, with the smaller numbers of individuals collected in the day, the ability to establish a statistical correlation between factors and larval density was limited. In another study, Hernandez et al. (2009) found that high turbulence in surface waters, caused by wind forcing, corresponded to ichthyoplankton's vertical movement to deeper waters. Substantial ship traffic is also responsible for increased turbidity, creating an artificial upwelling effect which resuspends sediment in the surrounding waters (Irvine et al. 1997, Lindholm et al. 2001). Finally dredging is another practice which increases the turbidity in the aquatic environment, as substrate is removed to increase depth for ship movement (Erftemeijer & Lewis 2006). As wind and ship traffic play an important role in coastal waters of Texas, the avoidance of turbulent surface waters could be an explanation for

ichthyoplankton vertical distributions. Turbulent waters are known to correspond to lower densities of larval fish, primarily because of reduced feeding success specifically in the coastal Texas area (Lunt & Smee 2014). Future research should be done on the effect of turbulent surface waters on ichthyoplankton movement, especially in the coastal Texas area.

Net avoidance and gear restrictions may further account for the low number of individuals collected during the day. In a study conducted by Thayer et al. (1983), it was found that higher densities of ichthyoplankton collected during the day, were obtained using a high-speed sampling technique rather than using a standard bongo net. During daylight hours larvae may easily be able to visual perceive the net and actively avoid the net due to slow standard sampling speeds. However, this theory assumes that (1) the larval fish are adequately developed to be able to swim faster than the sampling gear (2) the sampled waters have low turbidity values thus improving visual acuity, which was both not the case for this study.

Water property data (salinity, temperature, oxygen, and pH) indicated a mixed water column, for most sampling rounds. This does not support the SAAB Hypothesis in which ichthyoplankton use vertical salinity discrepancies to cue transportation and vertical movement. Although, there is the possibility that the salt wedge described in the SAAB Hypothesis did occur outside of the sampling area and therefore did cue larval transportation. From our results, we conclude that larvae are using the entire water column during incoming tides to be transported to the inshore nursery grounds, but can also be flushed out again if not settled properly with the outgoing tide as our results suggest.

III. Implications for possible environmental effects of desalination

Desalination plants require water intake systems and discharge system both of which result in harmful effects to the environment and thus unique management implications. Intake systems are placed in the aquatic environment and cause smaller organisms, such as ichthyoplankton, to be susceptible to impingement. In 2004, legislation was passed updating the requirements for existing facilities, which intake cooling waters, to reduce the mortality of impinged organisms of all life stages (USEPA 2004). Previously the industry standard was an intake mesh size of 9.5 mm which was solely aimed at reducing the impingement of adults and juvenile organisms and resulted in 80% or larger mortality rate of impinged ichthyoplankton (USAEPA 2004). These regulations are specified for cooling water intake systems which do not include desalination plants. As desalination is considered a newer methodology in the United States, many regulations are not yet specified to address the unique issues presented by desalination technology.

Desalination plants further require the placement of wastewater discharge systems. The wastewater produced is a warm briny solution often released at high velocities in attempts to acclimatize the wastewater with the environmental conditions. Ichthyoplankton are sensitive to changes in the environment including salinity, temperature, and current velocity as they are not yet fully developed and are experiencing a period of high growth rate.

We showed that larval fish occupy the whole water column in the Aransas Bay System as their presence in surface and non-surface tows showed. They were found in higher densities during the night, but also occurred during the day. They were present both during in- and outcoming tides and in all months sampled. With the known spawning seasonality of estuarine fish and shellfish species from the TPWD Coastal Fisheries monitoring program it is safe to expect that larvae are found in the inlet system throughout the year. Thus, the likelihood that

larval fish would encounter the brine effluent plume if a diffuser system was installed in the inlet channel is high. The same concerns apply for the intake system with the effect size dependent on the affected water volume.

Significantly larger densities of ichthyoplankton were found at non-surface depths, meaning that a discharge pipe with a diffusor located along the seafloor has the capacity to affect the majority of ichthyoplankton, particularly sciaenids. Locating the intake and the discharge out of the inlet and further offshore would reduce the possibility of negatively affecting the high concentration of ichthyoplankton traveling through inlets. If the discharge pipe is placed within an inlet, the restriction of discharge timing and depth could limit the negative effects to the ichthyoplankton.

IV. Summary & Conclusions

In coastal communities the revenue from fishing activities is vital to the economy. In coastal Texas species of particular economic importance belong to the family Sciaenidae (drums). Several sciaenid species such as *M. undulatus* and *S. ocellatus*, migrate offshore to spawn, once spawning is complete larvae are transported through coastal inlets into estuaries, and are also known as estuarian dependent species. The estuaries and bays act as critical nursery habitat which support the growth and development of the ichthyoplankton. The precise mechanism for larval transportation remains unclear, but from ichthyoplankton studies such as this we can gain a better understanding of the relationship between larval density and environmental factors. As desalination plants are increasingly proposed as a solution to the worlds growing freshwater crisis, so does their possible negative effects on the environment. Our results suggest that locating intake and discharge of a desalination plant in the coastal inlet channels would impact

larval stages of a diversity of fish species, with a considerable risk of negatively affecting recruitment processes. Species impacted would likely include important species for the commercial and recreational fishing industries.

References

Able, K.W., (2005). A re-examination of fish estuarine dependence: Evidence for connectivity between estuarine and ocean habitats. *Estuarian, Coastal, and Shelf Science 64*, 5-17

Anderson, J. T. (1988). A review of size dependent survival during pre-recruit stages of fishes in relation to recruitment. *Journal of Northwest Atlantic Fishery Science*, *8*, 55-66.

Baptista, V., Leitão, F., Morais, P., Teodósio, M. A., & Wolanski, E. (2020). Modelling the ingress of a temperate fish larva into a nursery coastal lagoon. *Estuarine, Coastal and Shelf Science*, *235*, 106601.

Boehlert, G. W., & Mundy, B. C. (1988). Roles of behavioral and physical factors in larval and juvenile fish recruitment to estuarine nursery areas. In *American Fisheries Society Symposium* (Vol. 3, No. 5, pp. 1-67).

Bromschwig, M. J. (2019). *Feeding Ecology of Ichthyoplankton at a Gulf of Mexico Coastal Inlet.* Master's thesis, Texas A&M University-Corpus Christi 64 pages.

Brown, C.A., Jackson, G.A., Holt, S.A., & Holt, G.J. (2005). Spatial and temporal patterns in modeled particle transport to estuarine habitat with comparisons to ichthyoplankton settlement patterns. *Estuarine, Coastal and Shelf Science 64*, 33–46. doi:10.1016/j.ecss.

Carreon-Martinez, L. B., Wellband, K. W., Johnson, T. B., Ludsin, S. A., & Heath, D. D. (2014). Novel molecular approach demonstrates that turbid river plumes reduce predation mortality on larval fish. *Molecular Ecology*, *23*(21), 5366-5377.

Collin, S. P., & Hart, N. S. (2015). Vision and photoentrainment in fishes: the effects of natural and anthropogenic perturbation. *Integrative Zoology*, *10*(1), 15-28.

Erftemeijer, P. LA, & Lewis III, R. R. R. (2006) "Environmental impacts of dredging on seagrasses: a review." *Marine pollution bulletin* 52.12: 1553-1572.

Faillettaz, R., Paris, C. B., & Irisson, J. O. (2018). Ichthyoplankton swimming behavior alters dispersal patterns from marine protected areas in the North-Western Mediterranean Sea. *Frontiers in Marine Science*, *5*, 97.

Fiksen, Ø., Aksnes, D. L., Flyum, M. H., & Giske, J. (2002). The influence of turbidity on growth and survival of fish larvae: a numerical analysis. In *Sustainable Increase of Marine Harvesting: Fundamental Mechanisms and New Concepts: Proceedings of the 1st Maricult Conference held in Trondheim, Norway, 25–28 June 2000* (pp. 49-59). Springer Netherlands.

Hankin, R. K. S. (2006). Special functions in R: introducing the gsl package. In *R News* (Vol. 6).

Hays, G. C. (2003). A review of the adaptive significance and ecosystem consequences of zooplankton diel vertical migrations. In *Migrations and Dispersal of Marine Organisms:*

Proceedings of the 37 European Marine Biology Symposium held in Reykjavík, Iceland, 5–9 August 2002 (pp. 163-170). Springer Netherlands.

Hernandez, F. J., Hare, J. A., & Fey, D. P. (2009). Evaluating diel, ontogenetic and environmental effects on ichthyoplankton vertical distribution using generalized additive models for location, scale and shape. *Fisheries Oceanography*, *18*(4), 224-236.

Holt, G., & Holt, S. (2000). Vertical distribution and the role of physical processes in the feeding dynamics of two larval sciaenids Sciaenops ocellatus and Cynoscion nebulosus. *Marine Ecology Progress Series 193*, 181–190. doi:10.3354/meps193181

Irvine K.N., Droppo I.G., Murphy T.P.,& Lawson A. (1997); Sediment Resuspension and Dissolved Oxygen Levels Associated with Ship Traffic: Implications for Habitat Remediation. *Water Quality Research Journal*; 32 (2): 421–438.

Kassambara, A. & Mundt, F. (2020) Factoextra: Extract and Visualize the Results of Multivariate Data Analyses. R Package Version 1.0.7. https://CRAN.R-project.org/package=factoextra

Lampert, W. (1989). The Adaptive Significance of Diel Vertical Migration of Zooplankton. *Functional Ecology*, *3*(1), 21–27. https://doi.org/10.2307/2389671

Lindholm, T., Svartström, M., Spoof, L., & Meriluoto, J. (2001). Effects of ship traffic on archipelago waters off the Långnäs harbour in Åland, SW Finland. *Hydrobiologia*, *444*, 217-225.

Lunt, J., & Smee, D. L. (2014). Turbidity influences trophic interactions in estuaries. *Limnology and Oceanography*, *59*(6), 2002-2012.

Minello, T.J. (1999). Nekton densities in shallow estuarine habitats of Texas and Louisiana and the identification of essential fish habitat. In *American Fisheries Society Symposium*, **22**, 43-75.

Miri, R., & Chouikhi, A. (2005). Ecotoxicological marine impacts from seawater desalination plants. *Desalination*,*182*(1-3), 403-410.

Missimer, T. M., & Maliva, R. G. (2018). Environmental issues in seawater reverse osmosis desalination: Intakes and outfalls. *Desalination*, *434*, 198-215.

Moustakas, C. T., Watanabe, W. O., & Copeland, K. A. (2004). Combined effects of photoperiod and salinity on growth, survival, and osmoregulatory ability of larval southern flounder Paralichthys lethostigma. *Aquaculture*, *229*(1-4), 159-179.

NOAA: National Marine Fisheries Service & Gulf States Marine Fisheries Commission (2001). SEAMAP Operations Manual for Collection of Data. National Centers for Environmental Information. https://www.nodc.noaa.gov/archive/arc0090/0150631/1.1/data/0-data/SEAMAP%20Ops%20MANUAL%202.pdf.

Pepin, P., Robert, D., Bouchard, C., Dower, J. F., Falardeau, M., Fortier, L., ... & Sponaugle, S. (2014). Once upon a larva: revisiting the relationship between feeding success and growth in fish larvae. *ICES Journal of Marine Science*, *72*(2), 359-373.

Petersen, K. L., Frank, H., Paytan, A., & Bar-Zeev, E. (2018). Impacts of seawater desalination on coastal environments. In *Sustainable desalination handbook* (pp. 437-463). Butterworth-Heinemann.

Pietrafesa, L. J., Janowitz, G. S., Brown, K. S., Askari, F., Gabriel, C., & Salzillo, L. A. (1988). The invasion of the Red Tide in North Carolina coastal waters.

Pinheiro, J., Bates, D., DebRoy, S., Sarkar, D., & R Core Team. (2021). *nlme: Linear and Nonlinear Mixed Effects Models*. https://CRAN.R-project.org/package=nlme

Rao, P., Morrow III, W. R., Aghajanzadeh, A., Sheaffer, P., Dollinger, C., Brueske, S., & Cresko, J. (2018). Energy considerations associated with increased adoption of seawater desalination in the United States. *Desalination*, *445*, 213-224.

R Core Team (2021). R: A language and environment for statistical computing. R Foundation for Statistical Computing, Vienna, Austria. URL https://www.R-project.org/.

RStudio Team (2020). RStudio: Integrated Development for R. RStudio, PBC, Boston, MA URL http://www.rstudio.com/.

Salonen, M., Urho, L., & Engström-Öst, J. (2009). Effects of turbidity and zooplankton availability on the condition and prey selection of pike larvae.

Schieler, B. M., Hale, E. A., & Targett, T. E. (2014). Daily variation in ingress of fall-spawned ichthyoplankton into Delaware Bay in relation to alongshore and along-estuary wind components. *Estuarine, Coastal and Shelf Science*, *151*, 141-147.

Seaberg, W. C. (1988). Observations on inlet flow patterns derived from numerical and physical model studies. In *Am. Fish Soc. Symp.* (Vol. 3, pp. 16-25).

Southwick Associates (2006). The 2006 economic benefits of hunting, fishing and wildlife watching in Texas. Southwick Associates Inc., Texas Parks & Wildlife Department.

Specker, J. L., Schreiber, A. M., McArdle, M. E., Poholek, A., Henderson, J., & Bengtson, D. A. (1999). Metamorphosis in summer flounder: effects of acclimation to low and high salinities. *Aquaculture*, *176*(1-2), 145-154.

Stunz, G. W., Coffey, D. M., & Seemann, F. (2022). *Benchmarking community structure of estuarine-dependent nekton near the Aransas Pass inlet*.

Teodósio, M.A., Paris, C.B., Wolanski, E., & Morais, P. (2016). Biophysical processes leading to the ingress of temperate fish larvae into estuarine nursery areas: A review. *Estuarine, Coastal and Shelf Science 183*, 187–202. doi:10.1016/j.ecss.2016.10.022

Thayer, G. W., Colby, D. R., Kjelson, M. A., & Weinstein, M. P. (1983). Estimates of larval-fish abundance: diurnal variation and influences of sampling gear and towing speed. *Transactions of the American Fisheries Society*, *112*(2B), 272-279.

Torres, P. (2020, April 13). *U.S. Army Corps of Engineers Awards Dredging Contract For Corpus Christi Ship Channel Improvement Project*. Port of Corpus Christi. https://portofcc.com/u-s-army-corps-of-engineers-awards-dredging-contract-for-corpus-christi-ship-channel-improvement-project/.

USEPA (US Environmental Protection Agency). (2004). National Pollutant Discharge Elimination System final regulations to establish requirements for cooling water intake

structures at Phase II existing facilities, Final Rule. *Federal Register*, *69*(131 (9 July 2004), 41575-41693.

Wang, D. P. (1988). Transport model for water exchange between coastal inlet and the open ocean. In *American Fisheries Society Symposium* (Vol. 3, pp. 9-15).

Weatherall, T.F., Scheef, L.P., & Buskey, E.J. (2018). Spatial and temporal settlement patterns of blue crab (*Callinectes sapidus* and *Callinectes similis*) megalopae in a drought-prone Texas estuary. *Estuarine, Coastal and Shelf Science 214*, 89–97. doi:10.1016/j.ecss.2018.09.017

Wenner, E. L., Knott, D. M., Barans, C. A., Wilde, S., Blanton, J. O., & Amft, J. (2005). Key factors influencing transport of white shrimp (*Litopenaeus setiferus*) post-larvae into the Ossabaw Sound system, Georgia, USA. *Fisheries Oceanography*, *14*(3), 175-194.

Wiseman Jr, W. J., & Dinnel, S. P. (1988). Shelf currents near the mouth of the Mississippi River. *Journal of physical oceanography*, *18*(9), 1287-1291.

Weinstein, MICHAEL P., et al. "Retention of three taxa of postlarval fishes in an intensively flushed tidal estuary, Cape Fear River, North Carolina." *Fishery Bulletin* 78.2 (1980): 419-436.

Whitfield, A. K., Potter, I. C., Neira, F. J., & Houde, E. D. (2023). Modes of ingress by larvae and juveniles of marine fishes into estuaries: From microtidal to macrotidal systems. *Fish and Fisheries*, *24*(3), 488-503.

Figures

Figure 1 Conceptual model displaying the response of three taxa (*Leiostomus xanthurus*, *Micropogonias undulatus*, and *Paralichthys* spp.) of ichthyoplankton to photoperiod and tidal flow. Taken from Weinstein et al. 1980.

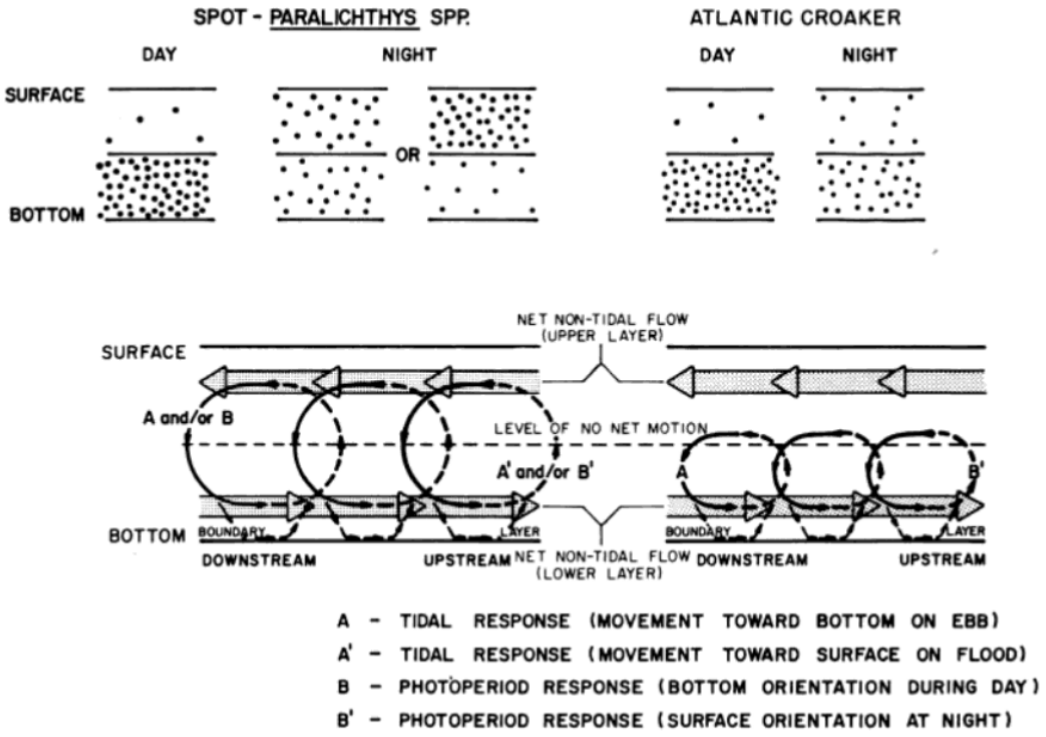

Figure 2: Map of sampling area in coastal Texas displaying sampling sites Corpus Christi Channel, Aransas Pass Channel, Lydia Ann Channel, and Port Aransas (CC1, AP1, LA1, & PA1 respectively). The blue diamond indicates the location of the proposed desalination plant.

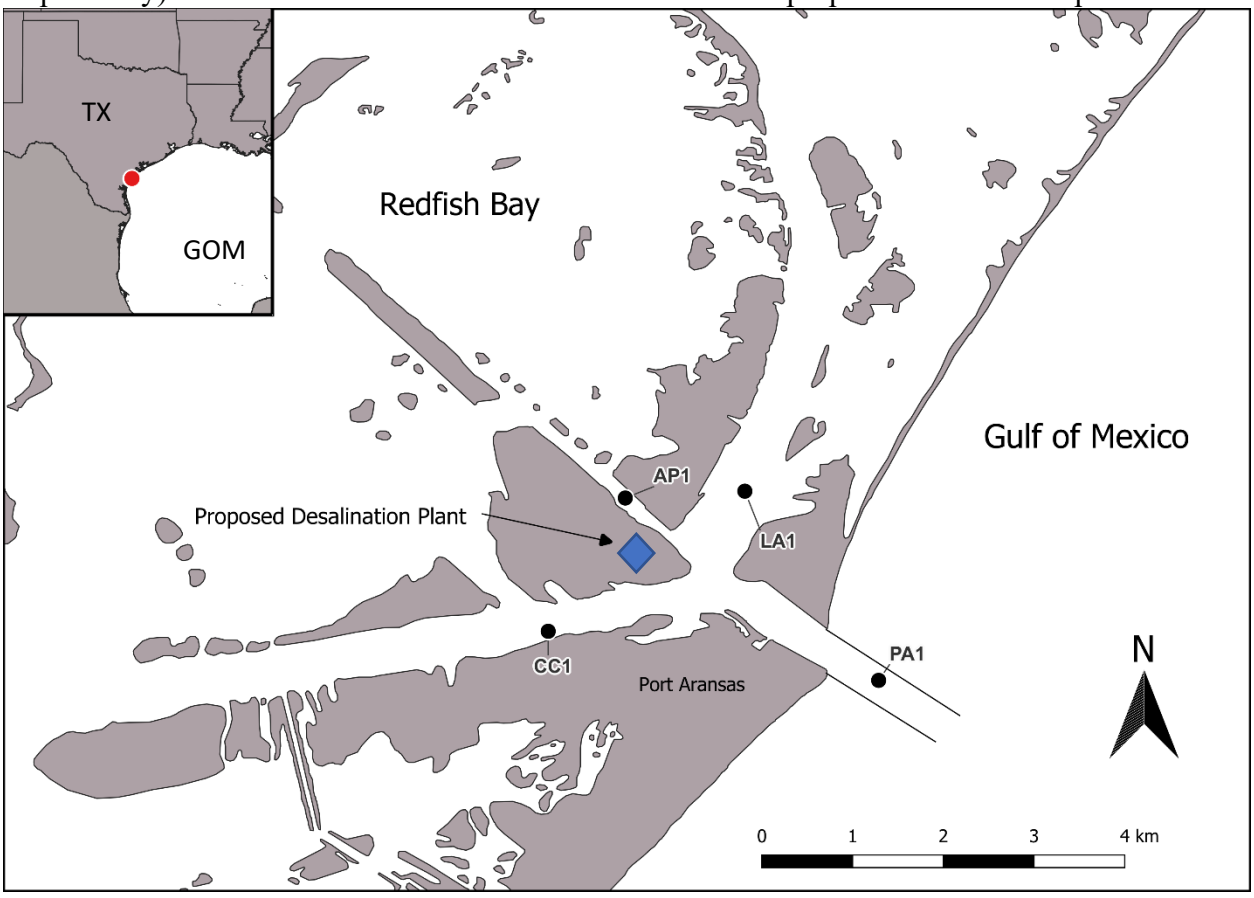

Figure 3: Depth profiles of temperature (° C) on the left-hand side and salinity (ppt) on the right-hand side arranged by sampling month. Profiles were taken for stations Corpus Christi (CC1), Aransas Pass (AP1), Lydia Ann (LA1), and Port Aransas (PA1) during day (D) and night (N) for ingoing (I) and outgoing (O) tides. June represented by A and B, October by C and D, November by E and F, and February by G and H.

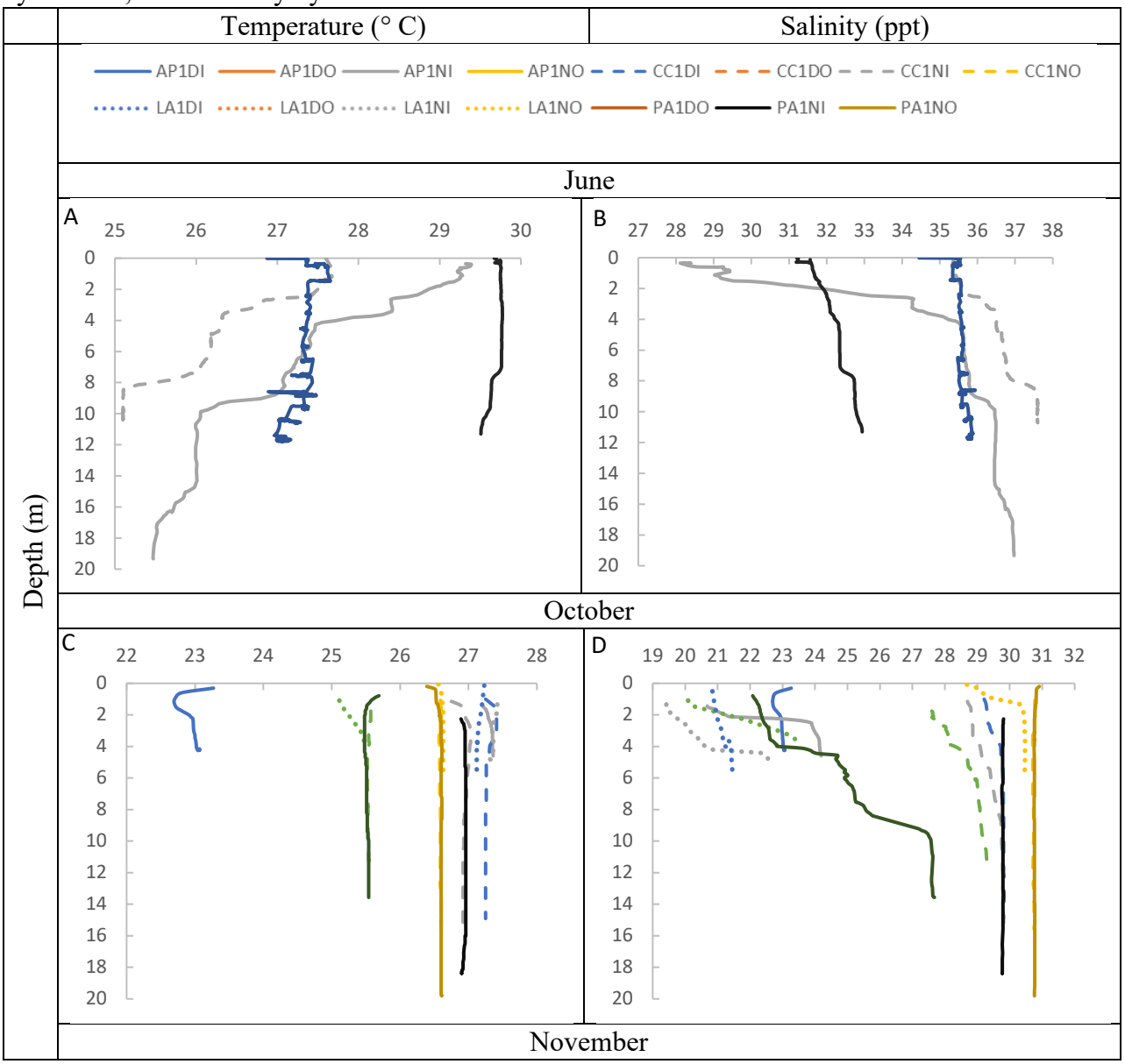

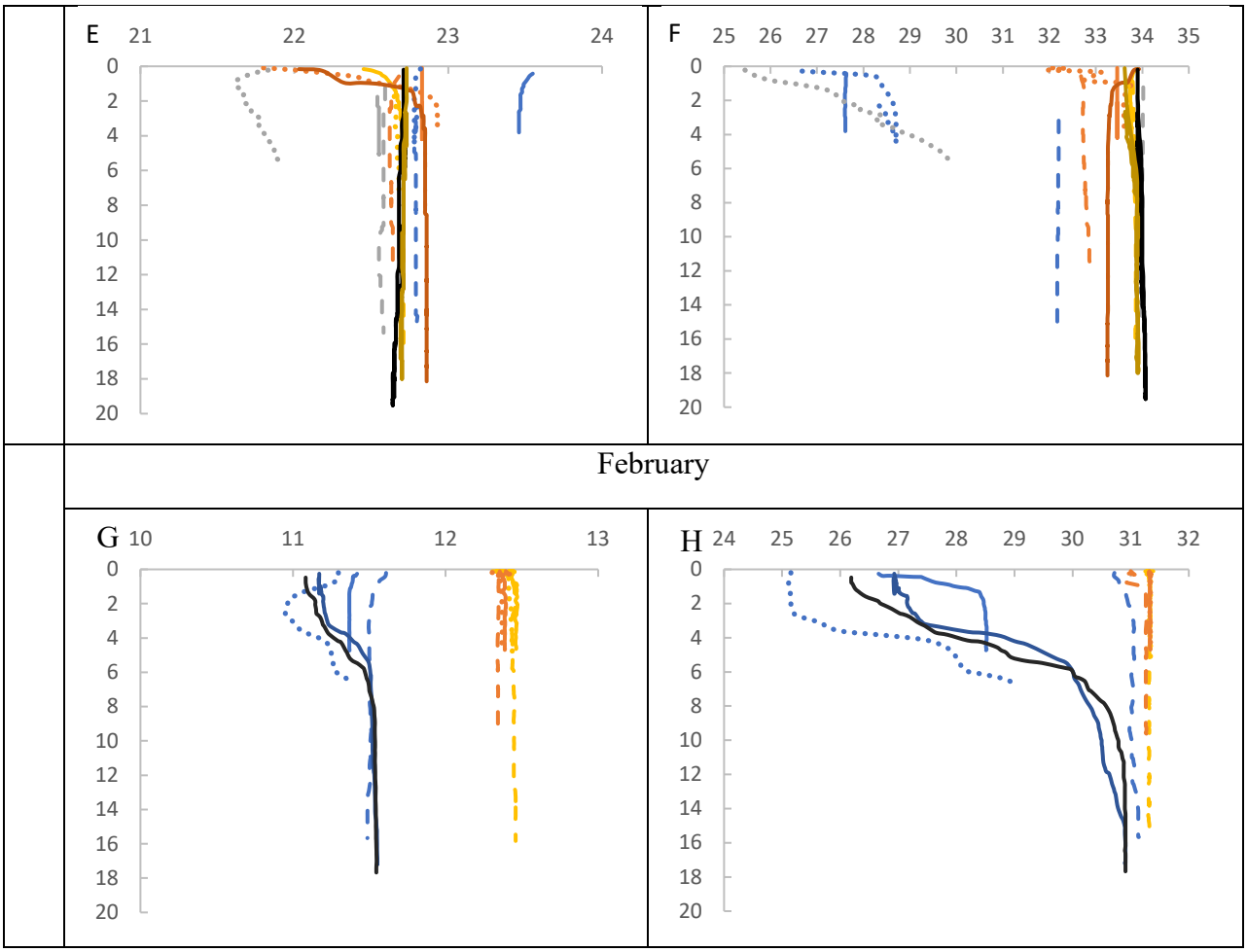
E
21
22
23
24
F
25
26
27
28
29
30
31
32
33
34
35
February
G
10
11
12
13
H
24
25
26
27
28
29
30
31
32

Figure 4: Depth profile of dissolved oxygen (DO) concentrations (mg/L) for sampling stations Corpus Christi night in (CCNI), Aransas Pass night in (AP1NI), Port Aransas night in (PA1NI), and Port Aransas day in (PA1DOI) taken during June.

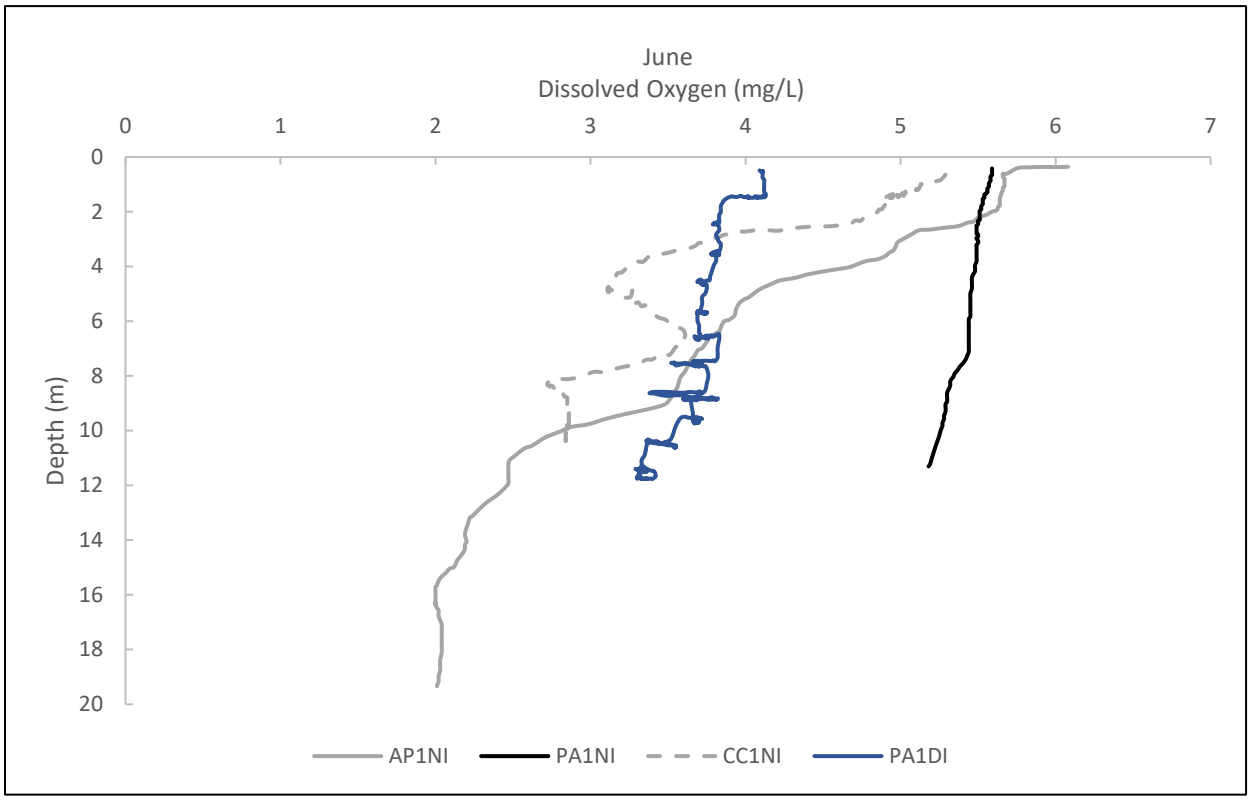

Figure 5: Data provided by NOAA (buoy station RTAT2) of surface water temperatures in the Corpus Christi Channel for the sample date of September 11th, 2022.

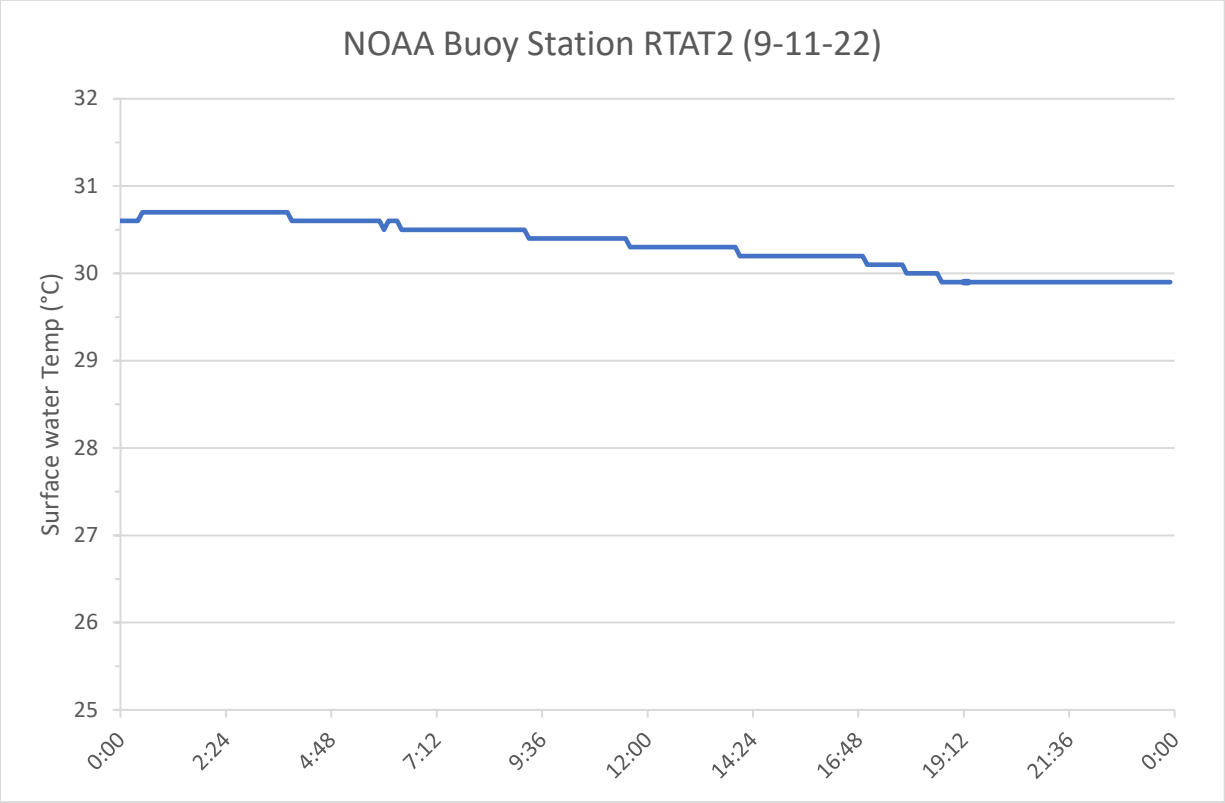

Figure 6: Median total ichthyoplankton densities (fish/ 100m^3) captured during the day (grey) and night (purple) for September, October, November, and February. Ichthyoplankton densities were log transformed. The lower and upper boxes correspond to the first and third quartiles, while the whiskers extend to no larger than 1.5 times the interquartile range (IQR). The black points indicated values that fell out of the IQR (outliers).

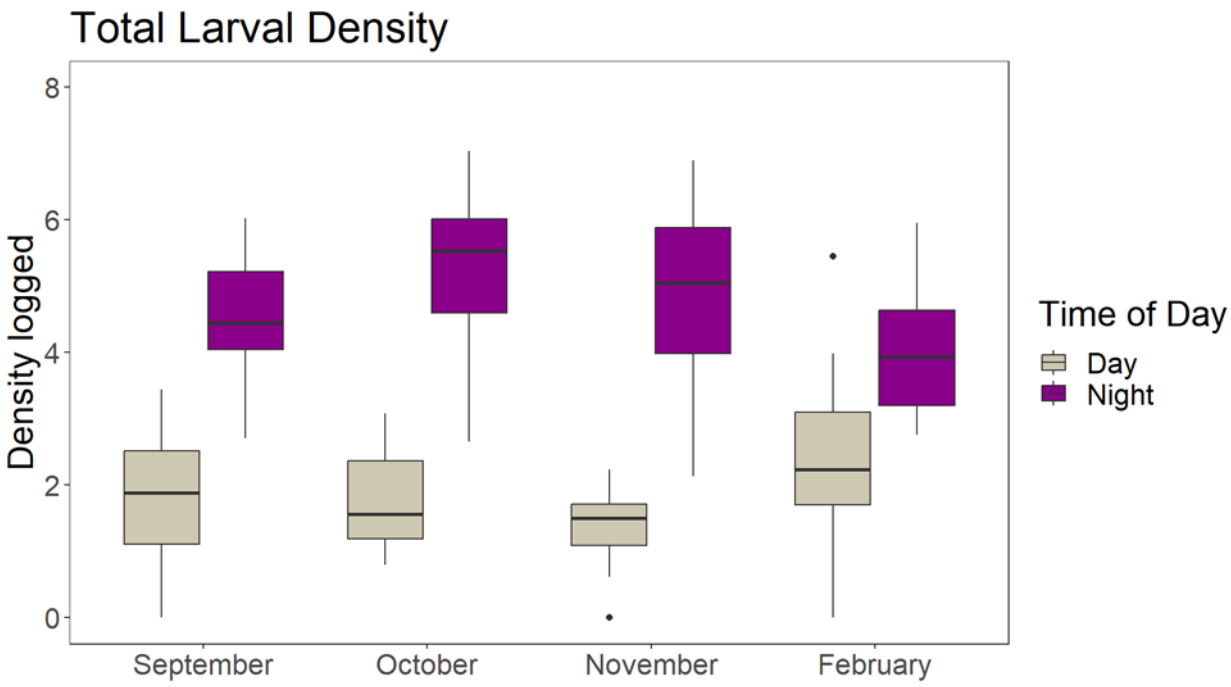

Figure 7: Median total ichthyoplankton densities (fish/ 100m^3) captured during ingoing tide (green) and outgoing tide (orange) for samples collected during the day. Ichthyoplankton densities were log transformed. The lower and upper boxes correspond to the first and third quartiles, while the whiskers extend to no larger than 1.5 times the interquartile range (IQR). The black points indicated values that fell out of the IQR (outliers).

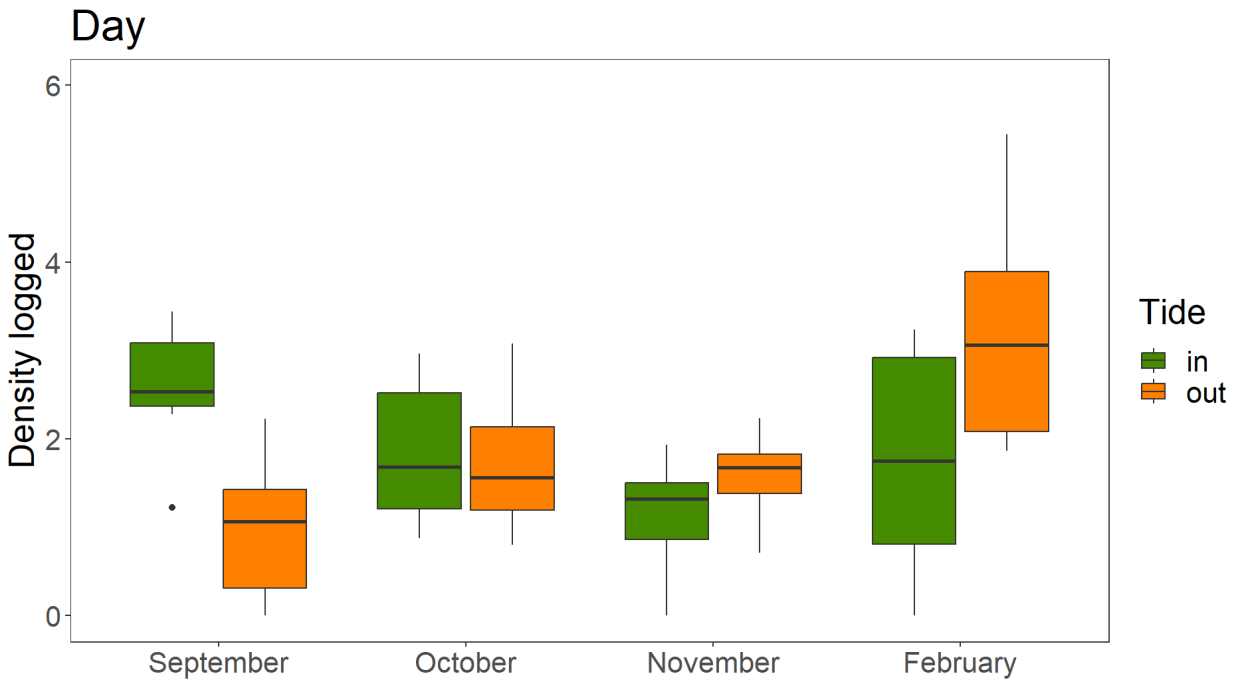

Figure 8: Median total ichthyoplankton densities (fish/ 100m^3) captured at surface depths (red) and non-surface depths (blue) for samples collected during the night. Ichthyoplankton densities were log transformed. The lower and upper boxes correspond to the first and third quartiles, while the whiskers extend to no larger than 1.5 times the interquartile range (IQR). The black points indicated values that fell out of the IQR (outliers).

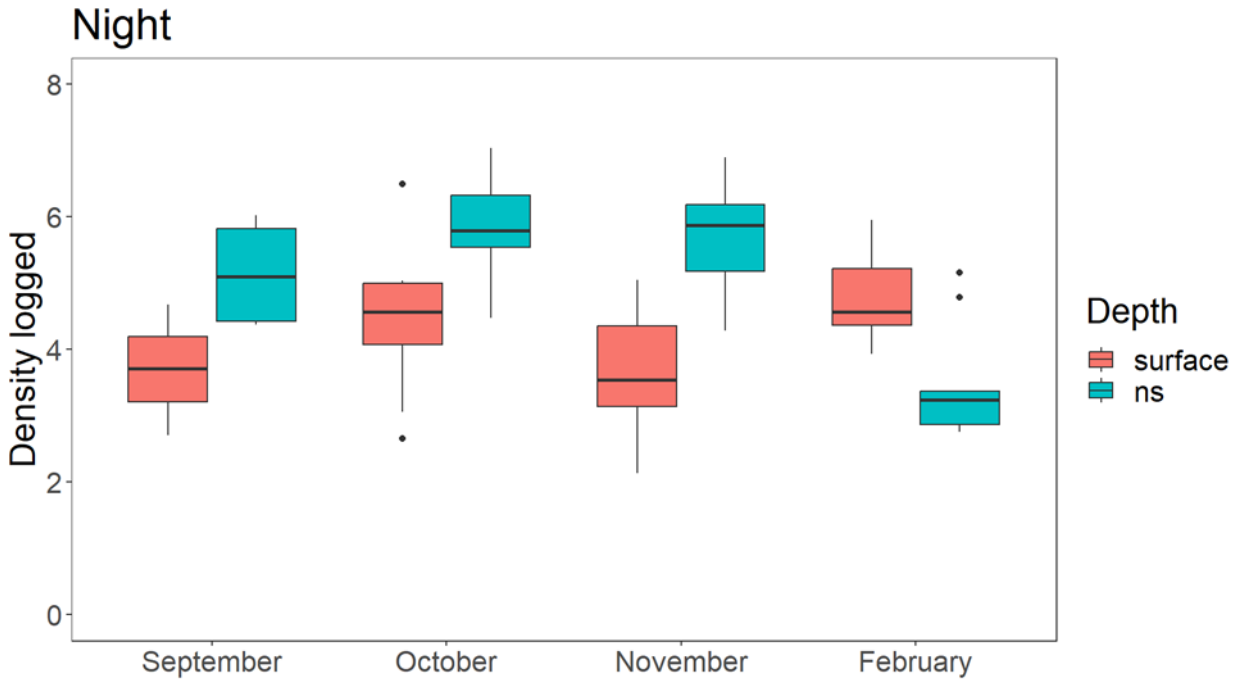

Figure 9: Median total sciaenid densities (fish/ 100m^3) captured at surface depths (red) and non-surface (ns) depths (blue). Sciaenid densities were log transformed with data restricted to fall months (September, October, and November). The lower and upper boxes correspond to the first and third quartiles, while the whiskers extend to no larger than 1.5 times the interquartile range (IQR). The black points indicated values that fell out of the IQR (outliers).

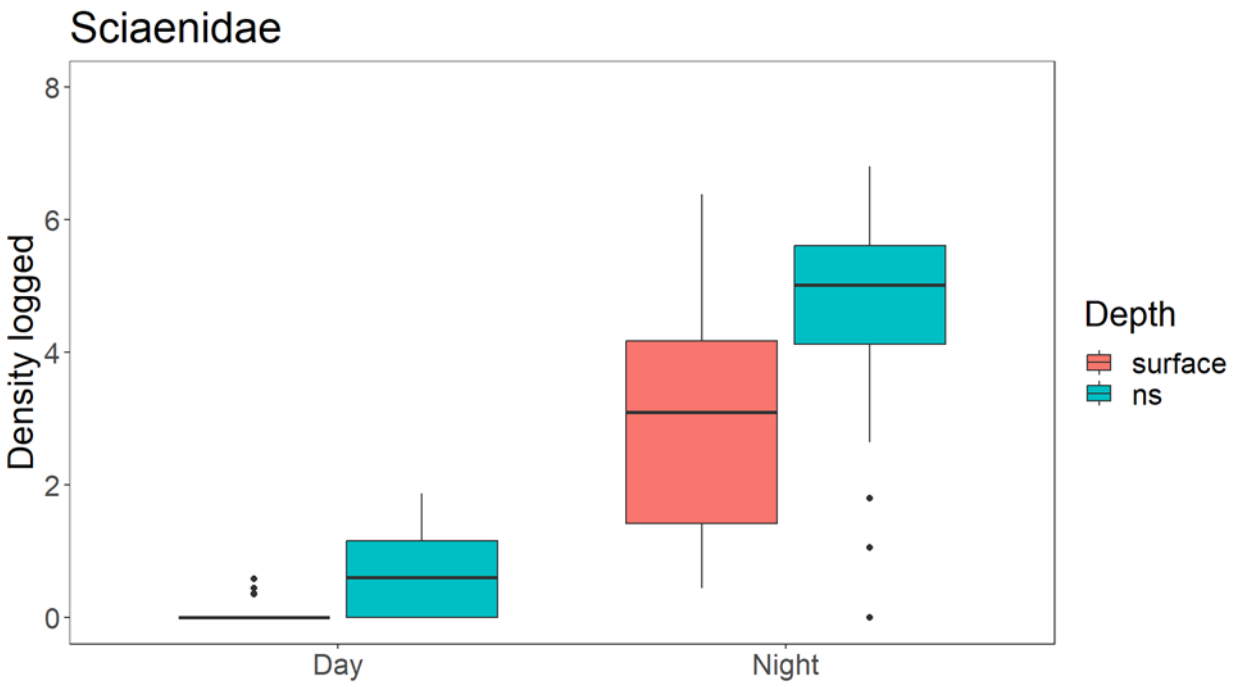

Figure 10: Median sciaenid densities (fish/ 100m^3) captured at surface depths (red) and non-surface depths (blue) for samples collected during the Day with data restricted to fall months (September, October, and November). Sciaenid densities were log transformed. The lower and upper boxes correspond to the first and third quartiles, while the whiskers extend to no larger than 1.5 times the interquartile range (IQR). The black points indicated values that fell out of the IQR (outliers).

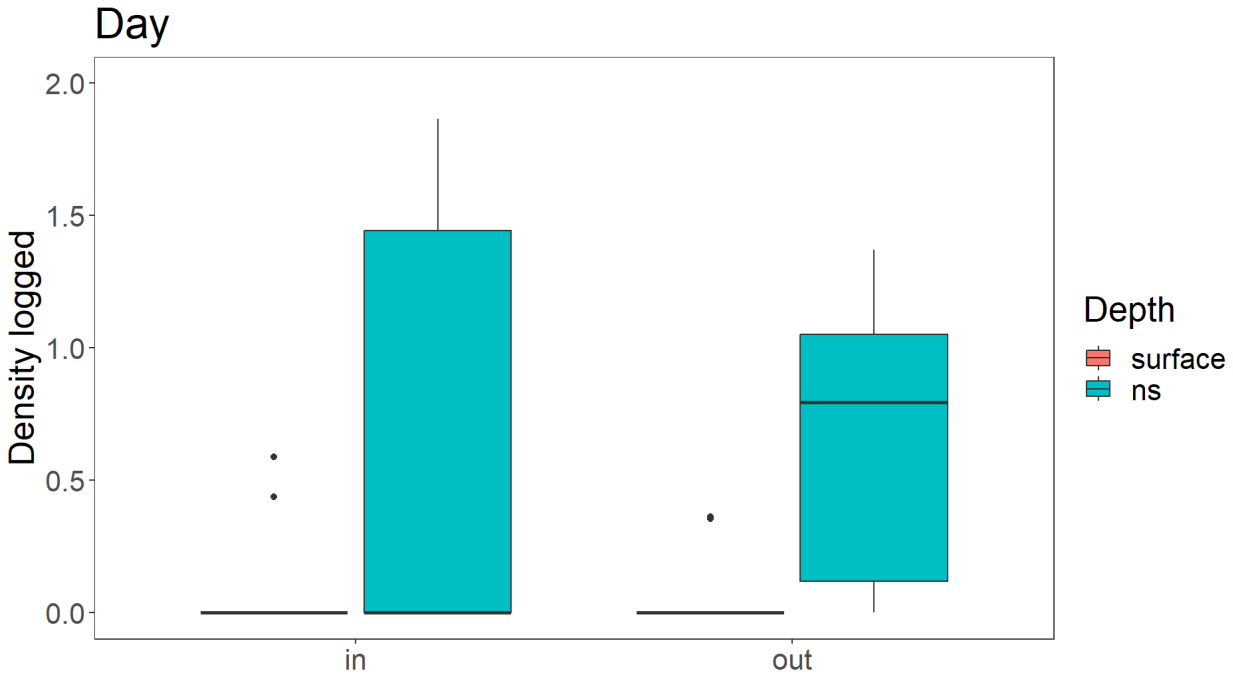

Figure 11: Median total sciaenid densities (fish/ 100m^3) captured at surface depths (red) and non-surface depths (blue) for samples collected during the night with data restricted to fall months (September, October, and November). Sciaenid densities were log transformed. The lower and upper boxes correspond to the first and third quartiles, while the whiskers extend to no larger than 1.5 times the interquartile range (IQR). The black points indicated values that fell out of the IQR (outliers).

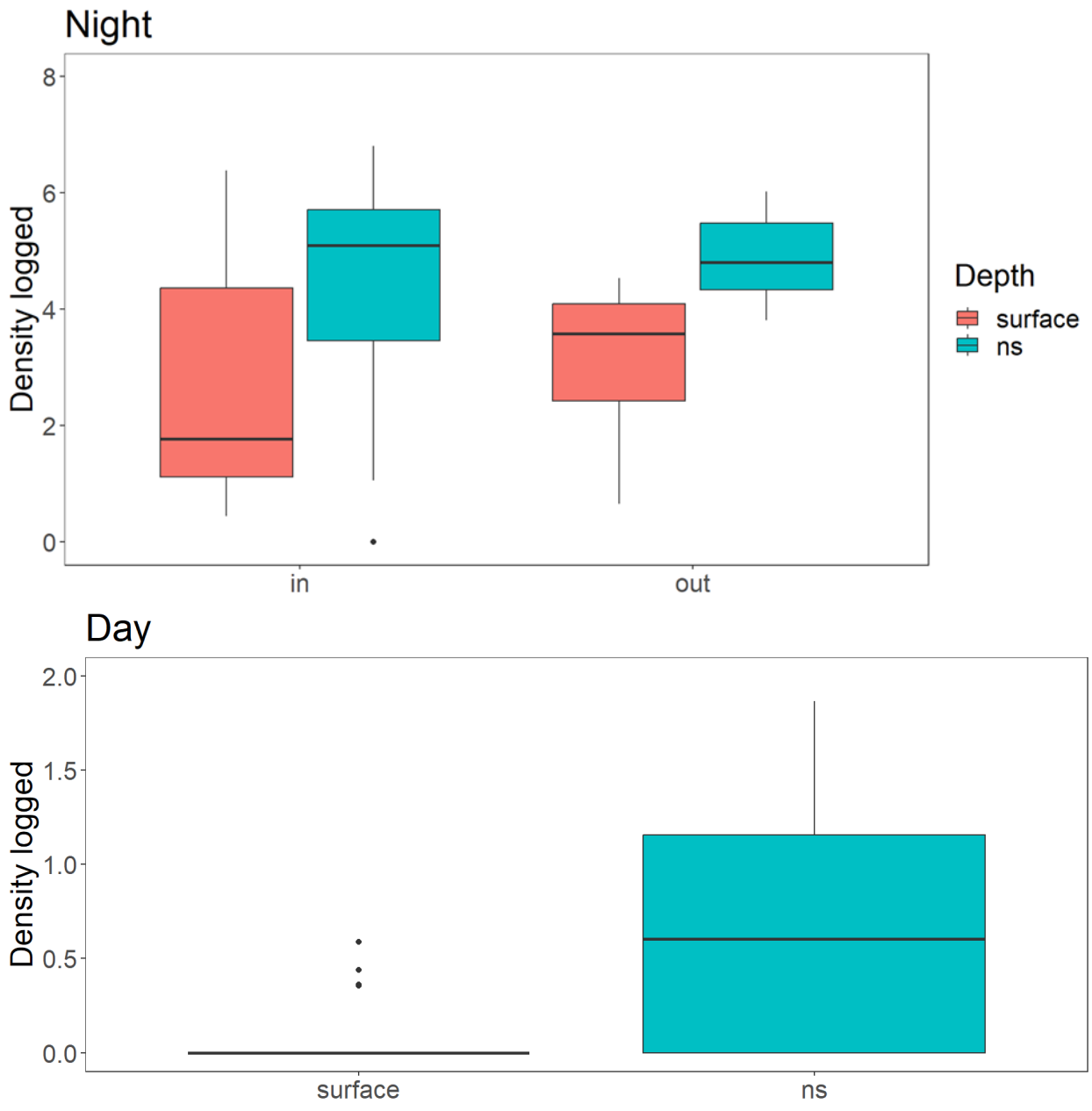

Figure 12: Scree plot of PCA of family densities. 83.5% of the variance in the data is explained by the first dimension. A total of 99.6% of the variance in the data is explained by the first four dimensions.

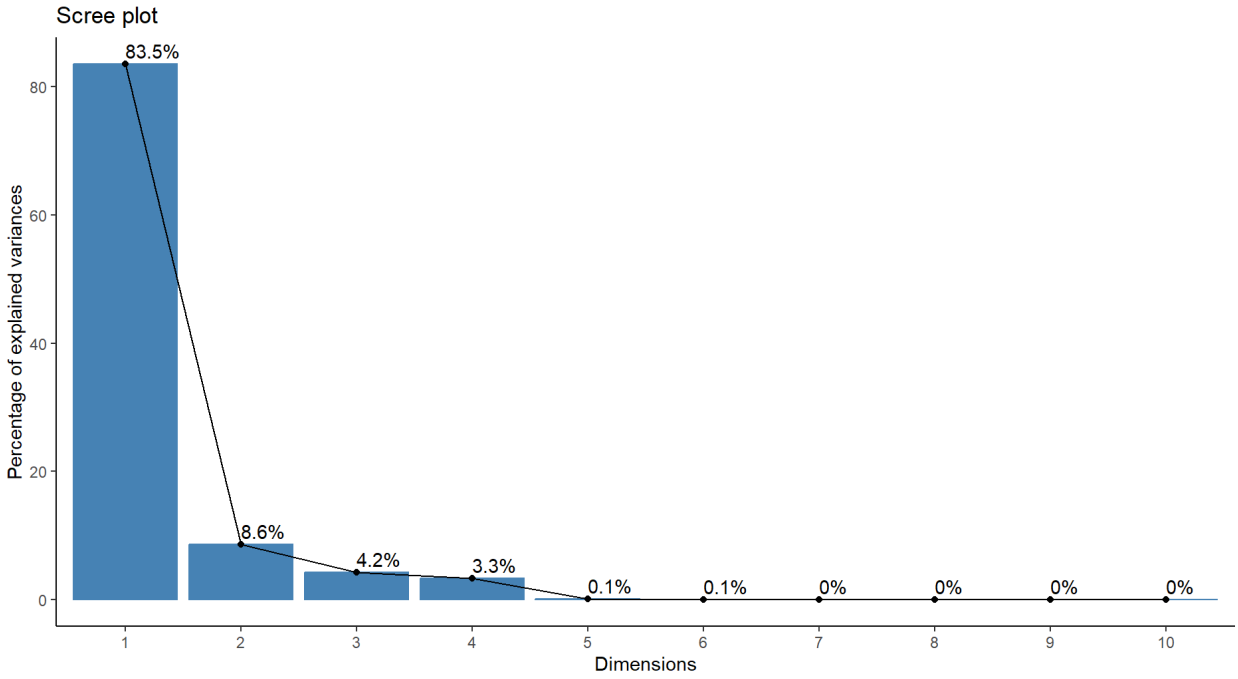

Figure 13: Loadings plot for principal component 1. Sciaenids, gobiids, and clupeids had the largest influence of PC1.

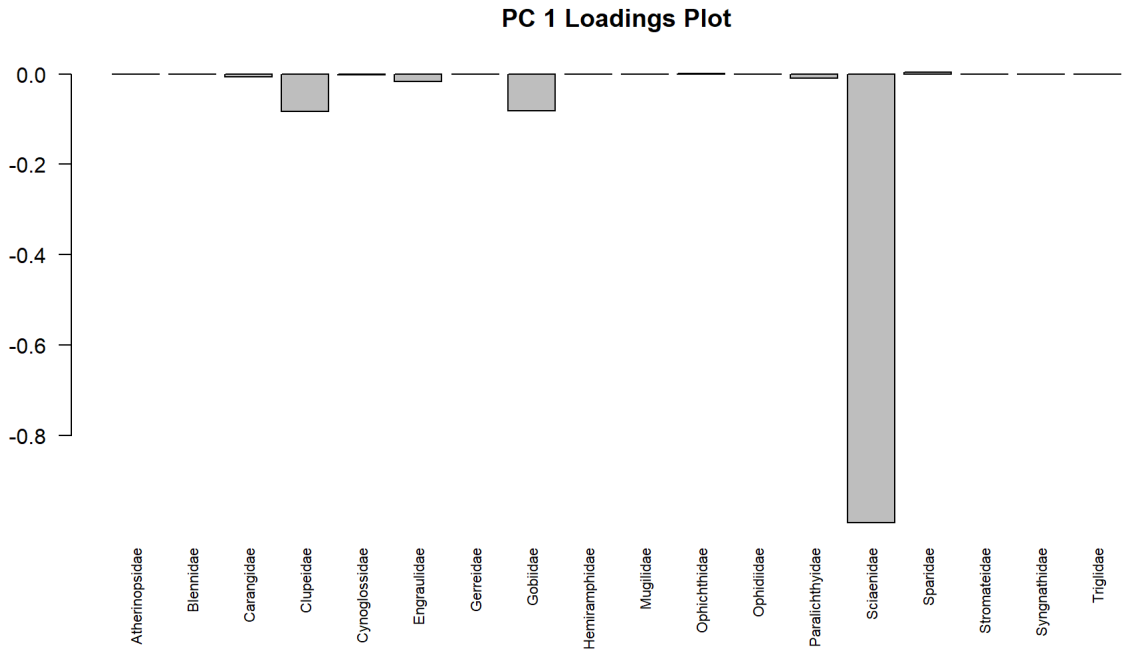

Figure 14: Loadings plot for principal component 2. Gobiids, clupeids, and sciaenids had the largest influence of PC2.

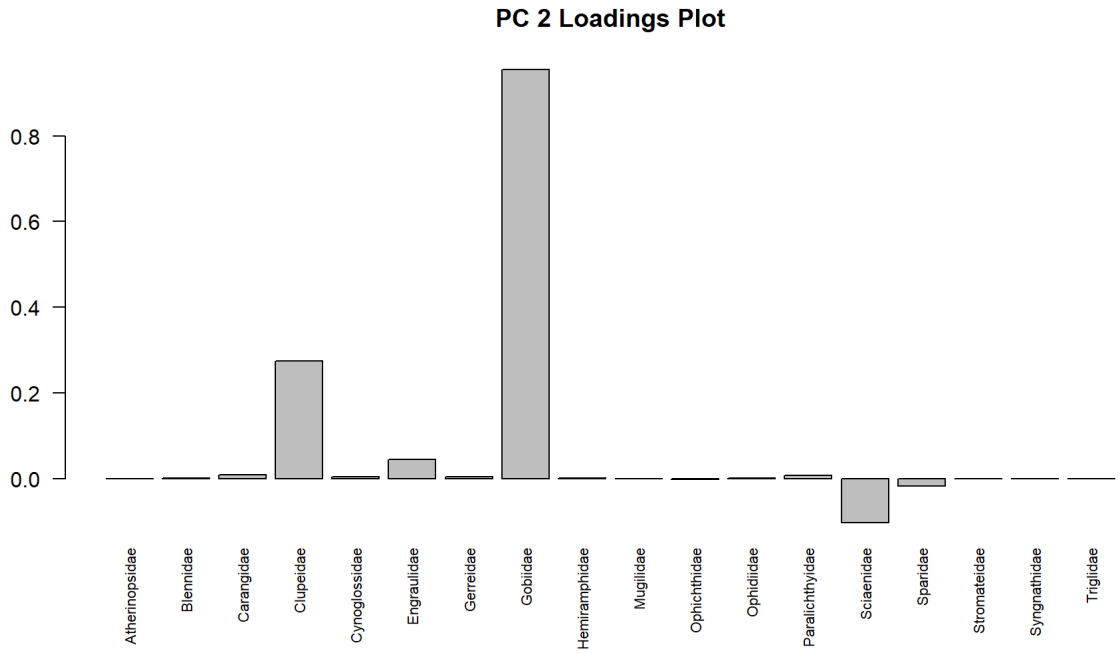

Figure 15: Loadings plot for principal component 3. Clupeids, sparids, and gobiids had the largest influence of PC3.

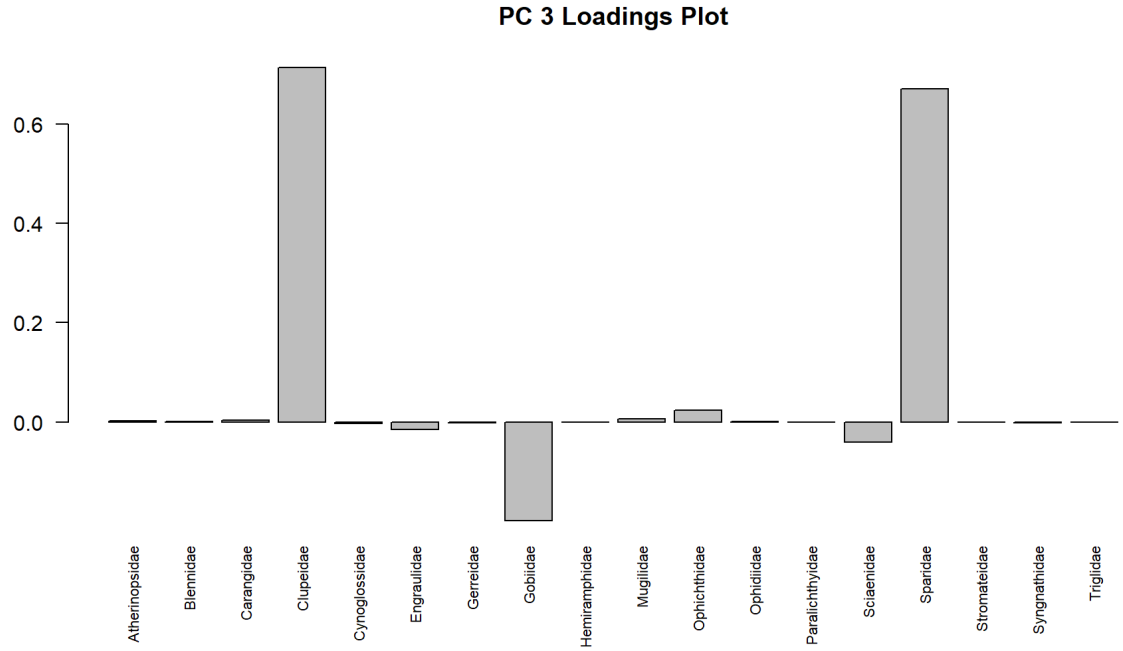

Figure 16: Loadings plot for principal component 4. Sparids, clupeids, and gobiids had the largest influence of PC4.

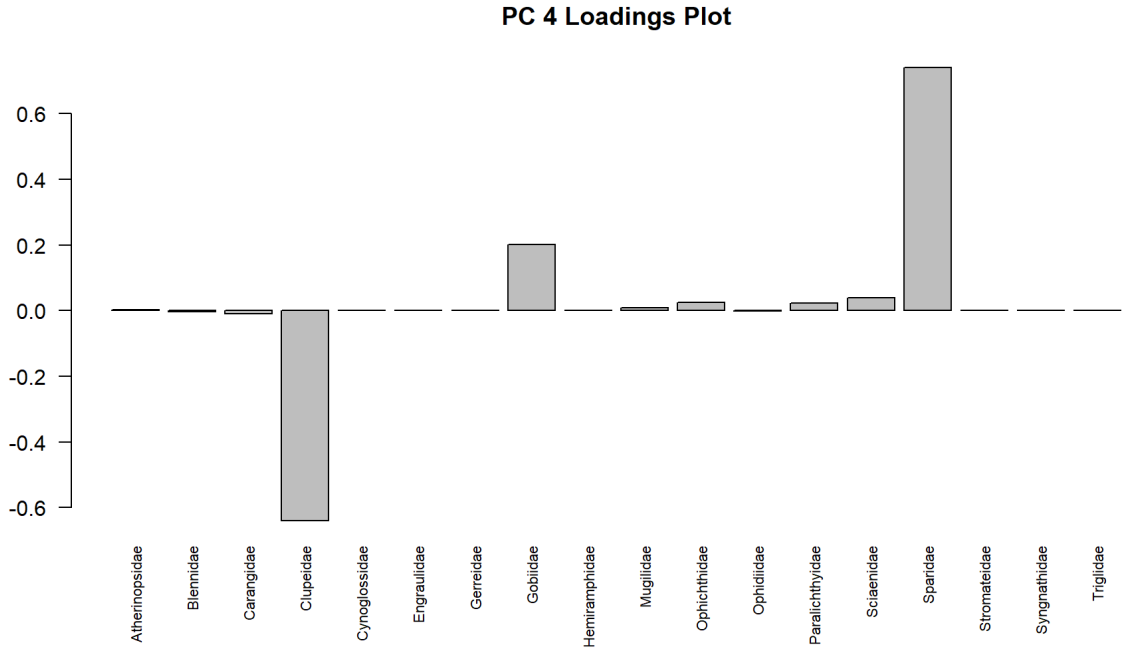

Figure 17: PCA biplot for PC1 and PC2. Points are colored by month (September, October, November, and February) and loading vectors indicate an increase in family density. Families displayed correspond to the families that contributed the most to PC1 and PC2.

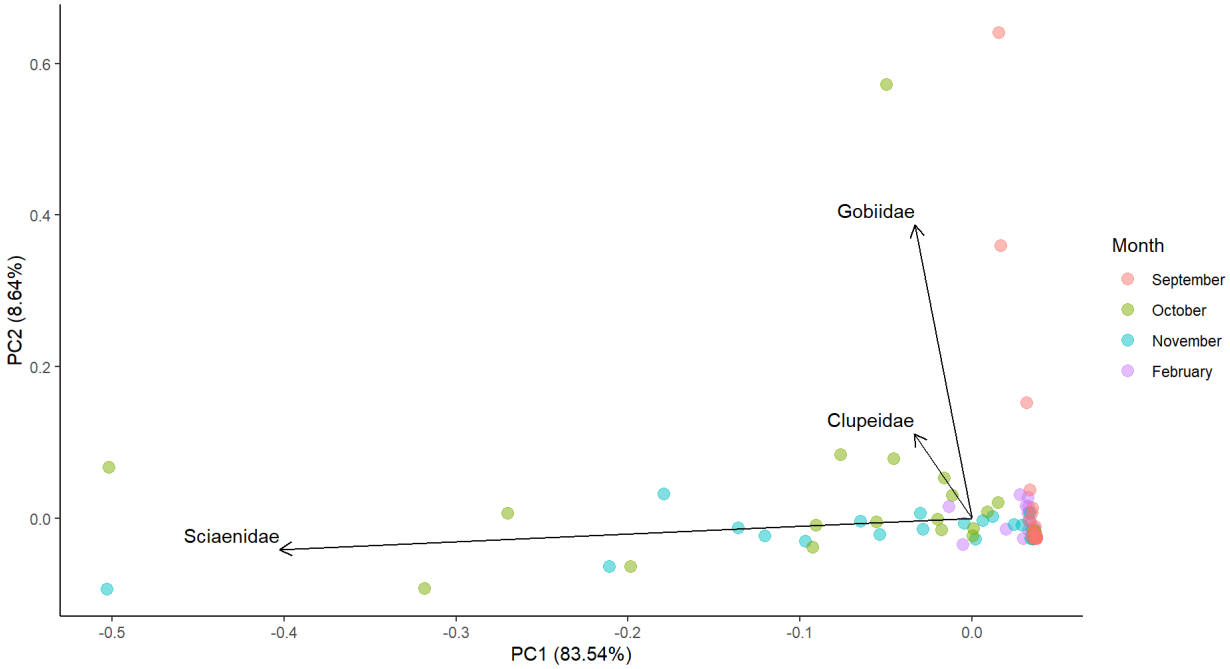

Figure 18: PCA biplot for PC3 and PC4. Points are colored by month (September, October, November, and February) and loading vectors indicate an increase in family density. Families displayed correspond to the families that contributed the most to PC3 and PC4.

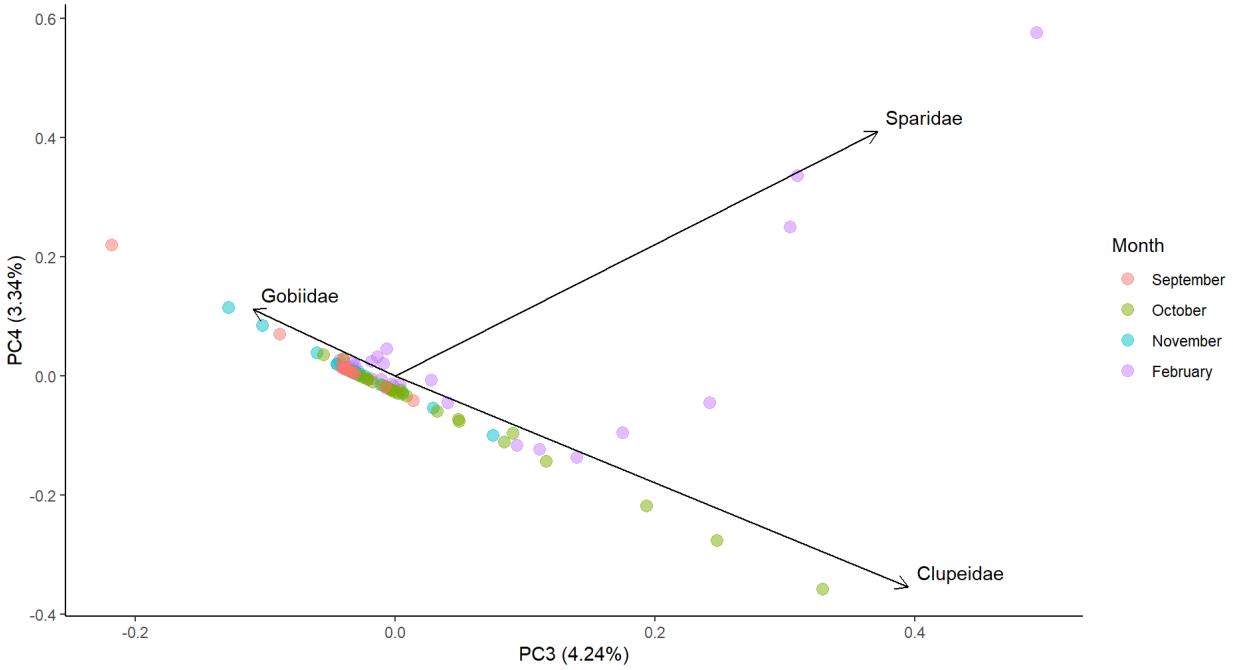

Figure 19: PCA biplot for PC1 and PC2. Points are colored by tidal cycle (ingoing and outgoing) and loading vectors indicate an increase in family density. Families displayed correspond to the families that contributed the most to PC1 and PC2.

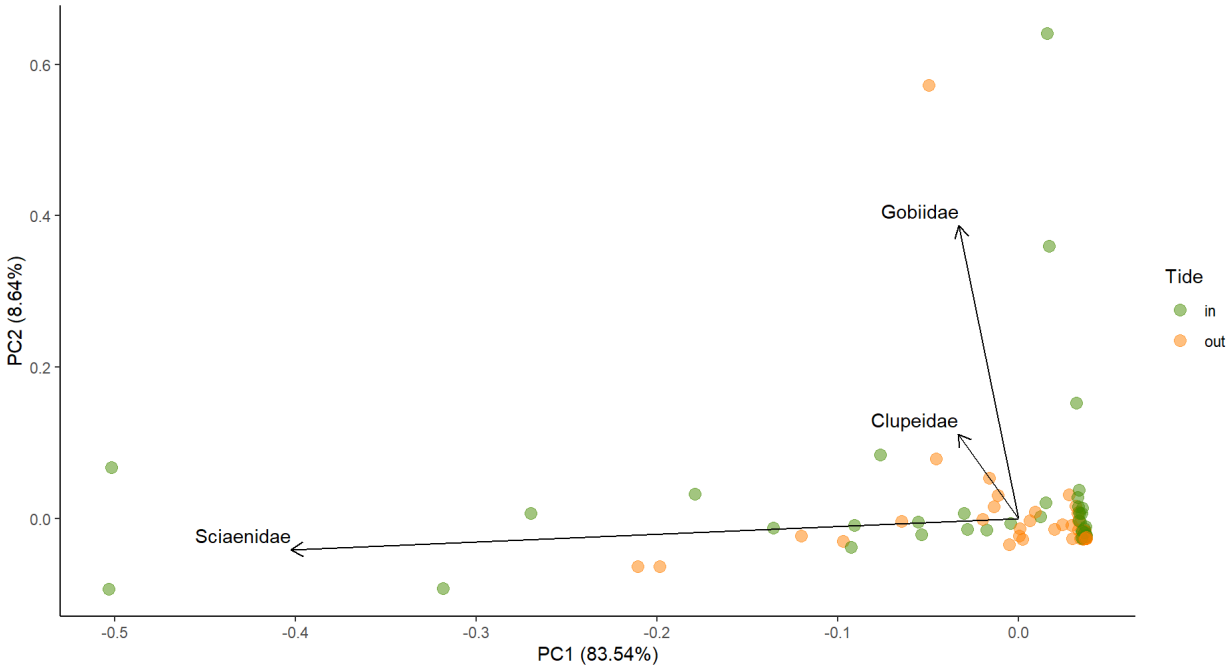

Figure 20: PCA biplot for PC3 and PC4. Points are colored by tidal cycle (ingoing and outgoing) and loading vectors indicate an increase in family density. Families displayed correspond to the families that contributed the most to PC3 and PC4.

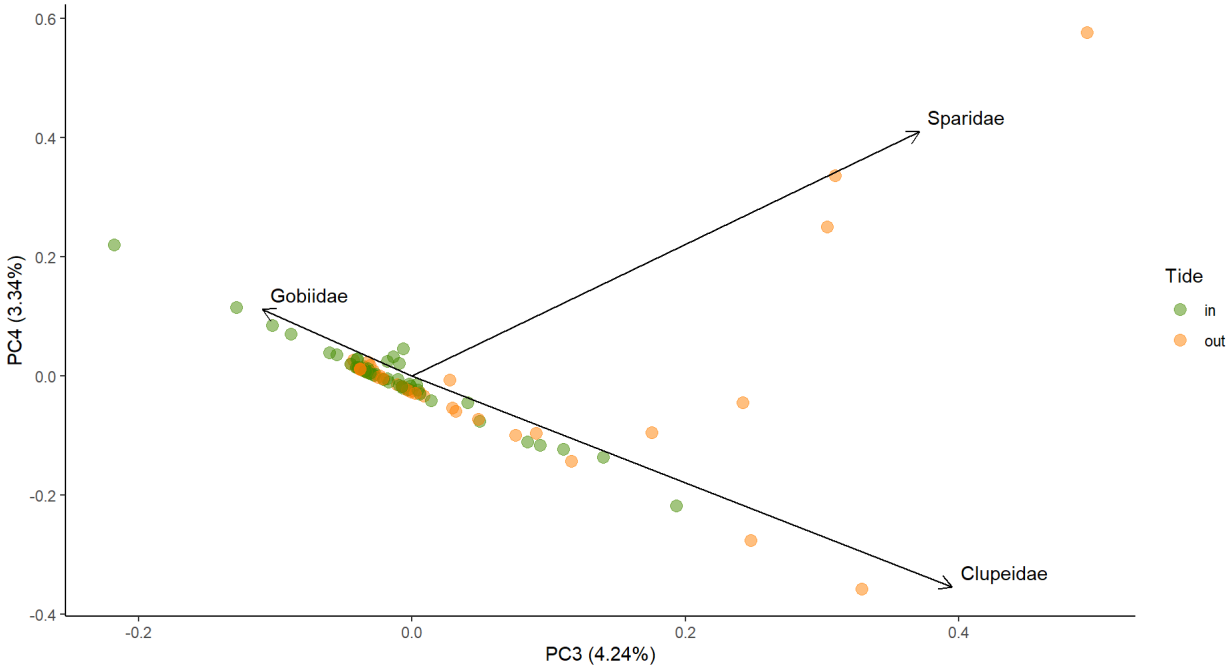

Figure 21: PCA biplot for PC1 and PC2. Points are colored by photoperiod (day and night) and loading vectors indicate an increase in family density. Families displayed correspond to the families that contributed the most to PC1 and PC2.

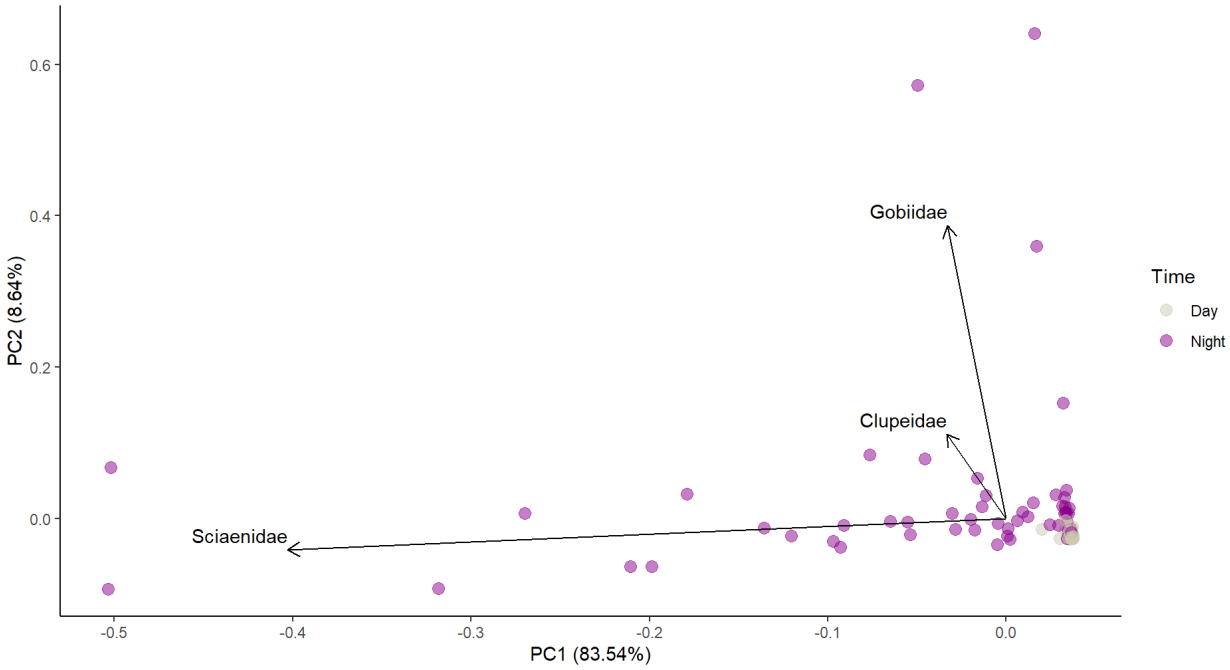

Figure 22: PCA biplot for PC3 and PC4. Points are colored by photoperiod (day and night) and loading vectors indicate an increase in family density. Families displayed correspond to the families that contributed the most to PC3 and PC4.

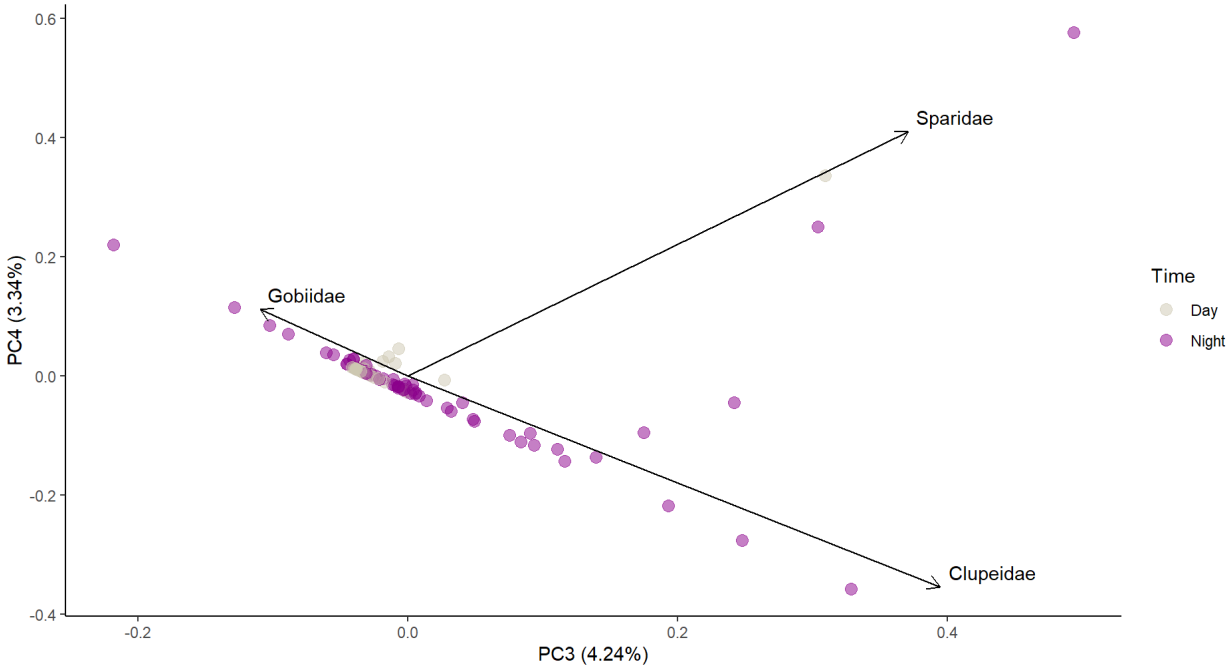

Figure 23: PCA biplot for PC1 and PC2. Points are colored by depth stratum (surface and non-surface) and loading vectors indicate an increase in family density. Families displayed correspond to the families that contributed the most to PC1 and PC2.

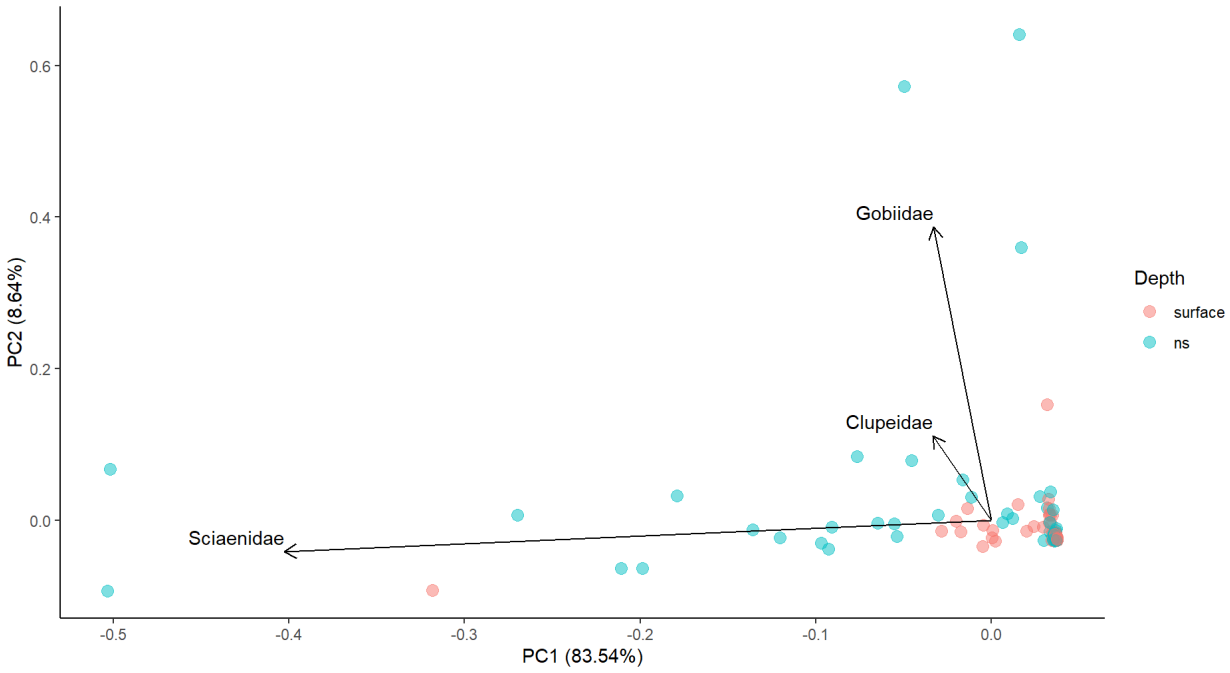

Figure 24: PCA biplot for PC3 and PC4. Points are colored by depth stratum (surface and non-surface) and loading vectors indicate an increase in family density. Families displayed correspond to the families that contributed the most to PC3 and PC4.

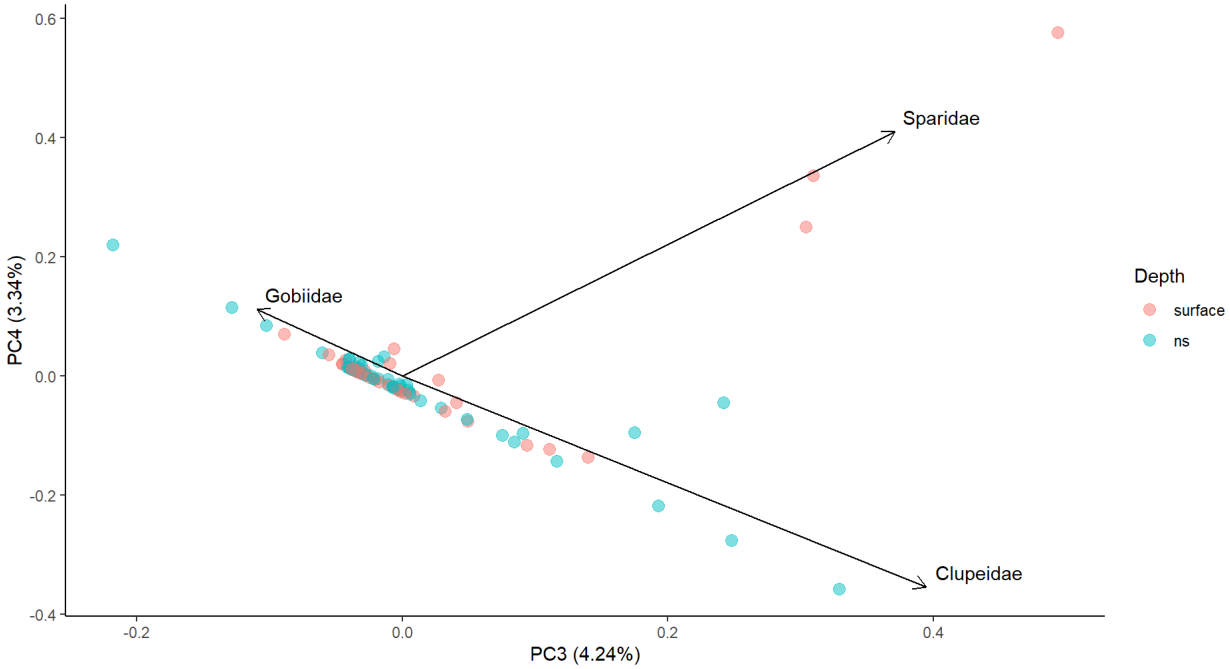

Tables

Table 1: Larval density (fish/100m^3) of families arranged by sampling month resulting in total averaged (mean ± standard deviation). Dash (-) denotes no taxa collected in tow.

	Month Larval Density (fish/100m^3)					
Family	June & July '21	September '21	October '21	November '21	February '22	Total Averaged (mean ± SD)
Archiridae	0.30	-	-	-	-	0.06 ± 0.37
Atherinopsidae	-	-	-	-	0.07	0.02 ± 0.12
Blennidae	0.34	0.51	0.32	-	-	0.22 ± 0.59
Carangidae	0.70	0.12	1.80	0.48	-	0.65 ± 1.81
Clupeidae	3.16	6.74	40.25	11.23	21.38	19.15 ± 33.94
Clupeiformes	8.36	2.50	4.13	0.83	0.03	2.51 ± 8.73
Cynoglossidae	0.39	0.25	0.51	0.29	-	0.30 ± 1.23
Engraulidae	1.97	5.91	2.61	1.52	-	2.05 ± 4.93
Gerreidae	3.40	0.38	0.06	0.20	-	0.77 ± 5.63
Gobiidae	10.68	36.35	18.50	10.54	2.67	14.71 ± 45.70
Hemiramphidae	0.25	0.08	-	-	-	0.06 ± 0.45
Lutjanidae	0.05	-	-	-	-	0.01 ± 0.08
Microdesmidae	0.17	-	-	-	-	0.02 ± 0.19
Mugilidae	-	-	-	-	0.19	0.04 ± 0.43
Ophichthidae	-	-	-	0.52	1.66	0.51 ± 2.07
Ophidiidae	-	-	0.15	0.06	0.07	0.07 ± 0.26
Paralichthyidae	0.26	0.67	0.91	2.18	4.18	1.85 ± 5.95
Sciaenidae	2.55	2.00	108.02	98.29	6.99	51.41 ± 138.77
Sparidae	0.08	-	-	0.01	22.64	5.32 ± 29.32
Stromateidae	-	-	0.03	0.01	-	0.01 ± 0.08

Syngnathidae	0.31	0.17	0.12	0.23	-	0.14	±	0.45
Triglidae	-	-	0.08	-	-	0.02	±	0.15
Unknown	10.28	0.08	0.05	0.09	0.02	1.10	±	11.37
Total	43.23	55.76	177.54	126.49	59.88	100.99		

Table 2: Larval density (fish/100m^3) of families arranged by sampling time (day or night) resulting in total averaged (mean ± standard deviation). Dash (-) denotes no taxa collected in tow.

	Time of Day Density (fish/100m^3)				
Family	Day	Night	Total Averaged (mean ± SD)		
Archiridae	0.03	0.08	0.06	±	0.37
Atherinopsidae	-	0.03	0.02	±	0.12
Blennidae	0.31	0.13	0.22	±	0.59
Carangidae	0.36	0.92	0.65	±	1.81
Clupeidae	2.90	33.91	19.15	±	33.94
Clupeiformes	0.46	4.37	2.51	±	8.73
Cynoglossidae	0.01	0.57	0.30	±	1.23
Engraulidae	0.45	3.51	2.05	±	4.93
Gerreidae	0.06	1.42	0.77	±	5.63
Gobiidae	0.89	27.27	14.71	±	45.70
Hemiramphidae	0.10	0.02	0.06	±	0.45
Lutjanidae	-	0.02	0.01	±	0.08
Microdesmidae	-	0.03	0.02	±	0.19
Mugilidae	-	0.08	0.04	±	0.43
Ophichthidae	0.23	0.76	0.51	±	2.07
Ophidiidae	-	0.13	0.07	±	0.26
Paralichthyidae	0.40	3.17	1.85	±	5.95
Sciaenidae	1.36	96.85	51.41	±	138.77
Sparidae	3.41	7.05	5.32	±	29.32
Stromateidae	0.01	0.01	0.01	±	0.08
Syngnathidae	0.17	0.10	0.14	±	0.45
Triglidae	-	0.04	0.02	±	0.15
Unknown	0.06	2.04	1.10	±	11.37
Total	11.20	182.51			

Table 3: Larval density (fish/100m^3) of families arranged by tidal cycle (ingoing or outgoing) resulting in total averaged (mean ± standard deviation). Dash (-) denotes no taxa collected in tow.

	Tide Larval Density (fish/100m^3)				
Family	in	out	Total Averaged (mean ± SD)		
Archiridae	0.10	-	0.06	±	0.37
Atherinopsidae	0.01	0.03	0.02	±	0.12
Blennidae	0.23	0.21	0.22	±	0.59
Carangidae	0.66	0.64	0.65	±	1.81
Clupeidae	15.04	25.49	19.15	±	33.94
Clupeiformes	2.44	2.63	2.51	±	8.73
Cynoglossidae	0.45	0.08	0.30	±	1.23
Engraulidae	2.89	0.75	2.05	±	4.93
Gerreidae	1.24	0.05	0.77	±	5.63
Gobiidae	18.21	9.32	14.71	±	45.70
Hemiramphidae	0.10	-	0.06	±	0.45
Lutjanidae	0.02	-	0.01	±	0.08
Microdesmidae	0.03	-	0.02	±	0.19
Mugilidae	0.01	0.09	0.04	±	0.43
Ophichthidae	0.22	0.96	0.51	±	2.07
Ophidiidae	0.05	0.09	0.07	±	0.26
Paralichthyidae	1.36	2.60	1.85	±	5.95
Sciaenidae	56.60	43.40	51.41	±	138.77
Sparidae	0.93	12.09	5.32	±	29.32
Stromateidae	0.01	0.01	0.01	±	0.08
Syngnathidae	0.15	0.11	0.14	±	0.45
Triglidae	0.03	-	0.02	±	0.15
Unknown	1.77	0.05	1.10	±	11.37
Total	102.55	98.59			

Table 4: Larval density (fish/100m^3) of families arranged by sampling depth (surface tow or not surface tow) resulting in total averaged (mean ± standard deviation). Dash (-) denotes no taxa collected in tow.

	Net Depth Larval Density (fish/100m^3)				
Family	surface	not surface	Total Averaged (mean ± SD)		
Archiridae	0.07	0.06	0.06	±	0.37
Atherinopsidae	0.04	0.01	0.02	±	0.12
Blennidae	0.22	0.23	0.22	±	0.59
Carangidae	0.59	0.70	0.65	±	1.81
Clupeidae	12.72	21.39	19.15	±	33.94
Clupeiformes	0.71	3.21	2.51	±	8.73
Cynoglossidae	0.02	0.39	0.30	±	1.23
Engraulidae	0.52	2.60	2.05	±	4.93
Gerreidae	1.35	0.59	0.77	±	5.63
Gobiidae	6.15	17.00	14.71	±	45.70
Hemiramphidae	0.07	0.06	0.06	±	0.45
Lutjanidae	-	0.01	0.01	±	0.08
Microdesmidae	-	0.02	0.02	±	0.19
Mugilidae	0.10	0.03	0.04	±	0.43
Ophichthidae	0.66	0.46	0.51	±	2.07
Ophidiidae	0.02	0.09	0.07	±	0.26
Paralichthyidae	1.67	1.96	1.85	±	5.95
Sciaenidae	22.93	64.28	51.41	±	138.77
Sparidae	10.41	3.66	5.32	±	29.32
Stromateidae	0.01	0.01	0.01	±	0.08
Syngnathidae	0.08	0.15	0.14	±	0.45
Triglidae	0.04	0.02	0.02	±	0.15
Unknown	2.21	0.77	1.10	±	11.37
Total	60.59	117.69			

Table 5: Sciaenid species density (fish/100m^3) arranged by sampling month resulting in total averaged (mean ± standard deviation). Dash (-) denotes no taxa collected in tow. Data is restricted to fall months: September, October, and November.

	Month Sciaenid Larval Density (fish/100m^3)					
sciaenid Spp.	September '21	October '21	November '21	Total Averaged (mean ± SD)		
Menticirrhus spp.	0.14	1.70	0.44	0.76	±	1.29
Cynoscion arenarius	-	0.31	-	0.12	±	0.41
Cynoscion nebulosus	0.66	-	-	0.15	±	0.62
Cynoscion nothus	0.08	0.65	0.02	0.28	±	0.95
Cynoscion spp.	-	0.15	0.03	0.07	±	0.42
Larimus fasciatus	-	0.26	0.25	0.20	±	0.58
Menticirrhus americanus	-	0.21	0.08	0.11	±	0.50
Micropogonias undulatus	0.04	92.74	94.28	71.92	±	165.22
Sciaenops ocellatus	0.76	8.73	0.22	3.71	±	9.55
Unknown	0.17	3.19	0.07	1.33	±	7.62
Total	1.86	107.94	95.40			

Table 6: Sciaenid species density (fish/100m^3) arranged by sampling time (day or night) resulting in total averaged (mean ± standard deviation). Dash (-) denotes no taxa collected in tow. Data is restricted to fall months: September, October, and November.

	Fall Time of Day Sciaenid Larval Density (fish/100m^3)		
	Day	Night	Total Averaged (mean ± SD)
sciaenid spp.			
Menticirrhus spp.	0.07	1.61	0.84 ± 1.29
Cynoscion arenarius	-	0.24	0.12 ± 0.41
Cynoscion nebulosus	0.16	0.14	0.15 ± 0.62
Cynoscion nothus	0.04	0.51	0.28 ± 0.95
Cynoscion spp.	0.04	0.10	0.07 ± 0.42
Larimus fasciatus	0.06	0.32	0.20 ± 0.58
Menticirrhus americanus	-	0.22	0.11 ± 0.50
Micropogonias undulatus	0.25	139.02	71.92 ± 165.22
Sciaenops ocellatus	0.09	7.10	3.71 ± 9.55
Unknown	0.02	2.55	1.33 ± 7.62
Total	0.73	151.83	

Table 7: Sciaenid species density (fish/100m^3) arranged by sampling depth (surface or not surface) resulting in total averaged (mean ± standard deviation). Dash (-) denotes no taxa collected in tow. Data presented is restricted to fall months: September, October, and November.

	Net Level Sciaenid Larval Density (fish/100m^3)		
	not surface	surface	Total Averaged (mean ± SD)
sciaenid Spp.			
Menticirrhus spp.	0.53	0.70	0.61 ± 1.29
Cynoscion arenarius	0.14	0.11	0.12 ± 0.41
Cynoscion nebulosus	0.24	0.04	0.15 ± 0.62
Cynoscion nothus	0.35	0.19	0.28 ± 0.95
Cynoscion spp.	0.10	0.03	0.07 ± 0.42
Larimus fasciatus	0.27	0.09	0.20 ± 0.58
Menticirrhus americanus	0.16	0.05	0.11 ± 0.50
Micropogonias undulatus	104.63	26.30	71.92 ± 165.22
Sciaenops ocellatus	3.75	3.66	3.71 ± 9.55
Unknown	1.77	0.72	1.33 ± 7.62
Total	111.92	31.89	

Table 8: Sciaenid species density (fish/100m^3) arranged by sampling tidal cycle (ingoing or outgoing) resulting in total averaged (mean ± standard deviation). Dash (-) denotes no taxa collected in tow. Data presented is restricted to the fall months: September, October, and November.

	Fall Tide Sciaenid Larval Density (fish/100m^3)				
	in	out	Total Averaged (mean ± SD)		
sciaenid spp.					
Menticirrhus spp.	0.41	0.98	0.70	±	1.29
Cynoscion arenarius	0.15	0.09	0.12	±	0.41
Cynoscion nebulosus	0.30	-	0.15	±	0.62
Cynoscion nothus	0.48	0.07	0.28	±	0.95
Cynoscion spp.	0.02	0.12	0.07	±	0.42
Larimus fasciatus	0.29	0.09	0.20	±	0.58
Menticirrhus americanus	0.12	0.11	0.11	±	0.50
Micropogonias undulatus	100.47	41.43	71.92	±	165.22
Sciaenops ocellatus	2.00	5.54	3.71	±	9.55
Unknown	0.19	2.55	1.33	±	7.62
Total	104.45	50.98			

Table 9: Morphological identification vs. genetic identification of paralichthyids from February sampling.

Vial	Morphological ID	Genetic ID	Identified Correctly
R1	*Paralichthys lethostigma*	*P. lethostigma*	Y
R2	*Paralichthys lethostigma*	*P. lethostigma*	Y
R3	*Paralichthys lethostigma*	*P. albigutta*	N
R4	*Paralichthys lethostigma*	*Citharichthys spilopterus*	N
R5	*Paralichthys lethostigma*	*Citharichthys spilopterus*	N
R6	*Paralichthys lethostigma*	*P. lethostigma*	Y
R7	*Paralichthys lethostigma*	*P. lethostigma*	Y
R8	*Citharichthys spilopterus*	*P. lethostigma*	Y
R9	*Paralichthys lethostigma*	*P. albigutta*	N
R10	*Paralichthys lethostigma*	*P. lethostigma*	Y
R11	*Paralichthys lethostigma*	*P. lethostigma*	Y
R12	*Paralichthys lethostigma*	*P. lethostigma*	Y
R13	*Paralichthys lethostigma*	*P. lethostigma*	Y
R14	*Paralichthys lethostigma*	*P. lethostigma*	Y
R15	*Citharichthys spilopterus*	*P. lethostigma*	N
R16	*Citharichthys spilopterus*	*P. lethostigma*	N
R17	*Paralichthys lethostigma*	*P. lethostigma*	Y
R18	*Paralichthys lethostigma*	*Citharichthys spilopterus*	N
R19	*Paralichthys lethostigma*	*P. lethostigma*	Y

Table 10: ANOVA model results for total larval density vs the factors month, time of day, depth of net, and tidal cycle. Showing degrees of freedom (df), *f*-value, and *p*-values.

Full Model Total Larval Density			
	df	*f*-value	*p*-value
(Intercept)	1	15.1003	0.000179
Month	3	4.6931	0.00408
Time_Day	1	35.2157	3.84E-08
Depth_Stratum	1	14.1094	0.000283
Tide	1	11.9995	0.000772
Month:Time_Day	3	9.2486	1.75E-05
Month:Depth_Stratum	3	9.8088	9.26E-06
Month:Tide	3	9.1405	1.99E-05
Time_Day:Depth_Stratum	1	8.8590	0.003621
Time_Day:Tide	1	1.0440	0.309246
Depth_Stratum:Tide	1	0.0486	0.825919

Table 11: ANOVA model results for total larval density collected during the day vs the factors month, depth of net, and tidal cycle. Showing degrees of freedom (df), *f*-value, and *p*-values.

Day Model: Total Larval Density			
	DF	*f*-value	*p*-value
(Intercept)	1	260.207	5.15E-21
Month	3	4.901	0.00473
Depth Stratum	1	0.0664	0.7976
Tide	1	0.0526	0.8195
Month:Depth Stratum	3	2.591	0.0635
Month:Tide	3	7.604	0.000294
Depth Stratum:Tide	1	0.5837	0.4485

Table 12: ANOVA model results for total larval density collected during the day grouped by month vs the factors of tidal cycle. Showing degrees of freedom (DF), *f*-value, and *p*-values.

Tide-Month Model: Total Larval Density			
	DF	*f*-value	*p*-value
September			
(Intercept)	1	72.807	1.93E-06
Tide	1	15.160	0.002135
October			
(Intercept)	1	77.863	4.30E-07
Tide	1	0.07784	0.7843
November			
(Intercept)	1	75.630	1.58E-06
Tide	1	1.9407	0.1888
February			
(Intercept)	1	61.853	1.06E-06
Tide	1	5.1574	0.0383

Table 13: ANOVA model results for total larval density collected during the night vs the factors month, depth of net, and tidal cycle. Showing degrees of freedom (DF), *f*-value, and *p*-values.

Night Model: Total Larval Density			
	DF	*f*-value	*p*-value
(Intercept)	1	1383.904	1.13E-40
Month	3	4.2133	0.009401
Depth Stratum	1	12.665	0.000776
Month:Depth Stratum	3	12.218	3.09E-06

Table 14: ANOVA model results for total larval density collected during the night grouped by month vs the factors of net depth. Showing degrees of freedom (DF), *f*-value, and *p*-values.

Month vs Depth Model: Total larval Density			
	DF	*f*-value	*p*-value
September			
(Intercept)	1	171.841	4.61E-05
Depth Stratum	1	4.3199	0.092243
October			
(Intercept)	1	97.738	4.69E-12
Depth Stratum	1	1.8018	0.187457
November			
(Intercept)	1	126.256	2.52E-13
Depth Stratum	1	0.7472	0.393059
February			
(Intercept)	1	132.285	6.65E-13
Depth Stratum	1	1.5710	0.219136

Table 15: ANOVA model results for Sciaenid larval density vs the factors month, time of day, depth of net, and tidal cycle. Showing degrees of freedom (DF), f-value, and p-values.

Full Model: Sciaenidae Larval Density			
	DF	*f*-value	*p*-value
(Intercept)	1	3.05642	0.084116
Time of Day	1	75.772	2.55E-13
Depth	1	1.1316	0.290516
Tide	1	0.01159	0.9145
Time of Day:Depth	1	4.86152	0.0302
Time of Day:Tide	1	0.59634	0.4421
Depth:Tide	1	0.02150	0.8837

Table 16: ANOVA model results for sciaenid larval density collected during the day vs the factors depth of net and tidal cycle. Showing degrees of freedom (DF), *f*-value, and *p*-values.

Day Model: Sciaenidae Larval Density			
	DF	*f*-value	*p*-value
(Intercept)	1	16.4154	0.000228
Depth	1	4.91036	0.03244
Tide	1	0.07799	0.78146
Depth:Tide	1	0.10339	0.74947

Table 17: ANOVA model results for Sciaenid larval density collected during the night vs the factors depth of net and tidal cycle. Showing degrees of freedom (DF), *f*-value, and *p*-values.

Night Model: Sciaenidae Larval Density

	DF	*f*-value	*p*-value
(Intercept)	1	28.4093	3.62E-06
Depth	1	6.649254	0.013515
Tide	1	0.249226	0.620226
Depth:Tide	1	0.003386	0.953872